Geology, Geophysics & Environment 2025, vol. 51 (4): 337–360

# Assessment of the geogenic salinity conditions in the hyporheic zone of the Moszczenica River in the Rogóźno salt dome zone (Zgierz district) based on radium isotopes

Maciej Ziułkiewicz[1], Paweł Grabowski[2], Magdalena Długosz-Lisiecka[3]

*[1] University of Lodz, Faculty of Geographical Sciences, Department of Geology and Geomorphology, Łódź, Poland, e-mail: maciej.ziulkiewicz@geo.uni.lodz.pl (corresponding author), ORCID ID: 0000-0002-9196-845X*
*[2] Warsaw University of Technology, Faculty of Civil Engineering, Mechanics and Petrochemistry, Płock, Poland, e-mail: pawel.grabowski@pw.edu.pl, ORCID ID: 0000-0001-8918-4624*
*[3] Lodz University of Technology, Institute of Applied Radiation Chemistry, Łódź, Poland, e-mail: magdalena.dlugosz@p.lodz.pl, ORCID ID: 0000-0003-1358-049X*

Received: 16 June 2025; accepted: 6 November 2025; first published online: 22 December 2025

---

***Abstract:*** On the border of the Kujavian Anticlinorium and the Łódź Synclinorium, the Rogóźno salt dome was formed and broke through the overburden of Mesozoic formations. The groundwater circulating around them leaches the salt body and, being saline, is subject to drainage in the Moszczenica valley. Previous measurements of vertical hydraulic gradients and physicochemical analyses showed conditions favorable for the penetration of aqueous solutions of Zechstein salt into the riverbed, which is particularly intensified at low surface water levels. The main objective of this publication is to determine the origin of groundwater flowing into the hyporheic zone (HZ) of Moszczenica using radium isotopes. Hydrochemical studies were carried out on deep groundwater in the supply area, flow and drainage zones of the Groundwater Body, within the boundaries of which the salt dome is located. The preliminary assessment of the hydrochemical specificity of HZ waters, carried out using the EMMA method, showed that these are waters which, as a mixture, cannot be related to any of the end member elements selected from the set of local groundwaters. Based on previous hydrochemical studies, the share of deep groundwaters in the HZ was determined to be 22–33%. On this basis, the reconstruction of the sought mixing end element was performed with the isotopic signature of the river water and the mixture of HZ waters. Using several computational scenarios, it was indicated that these may be waters from deep parts adjacent to the salt diapir of Cretaceous aquifers from the southwest.

***Keywords:*** salt diapir, ascension, vertical hydraulic gradient, the Łódź Synclinorium, EMMA method

---

## INTRODUCTION

The ascension of salty underground waters has been known in central Poland since the times of the first settled cultures (Bukowski 1963, Jodłowski 1977). The local tradition of salt-making is recorded in the names of today's localities, which date back to the oldest mentions in written historical sources. However, in the area that became the object of this research, this type of tradition does not occur. Despite its rich economic history (Kamiński 1993), there is no evidence of prehistoric salt production. The places of the occurrence of salt flats and salt-loving plants mentioned by Jaworski (1964) were the result of extensive geological exploration works.

https://doi.org/10.7494/geol.2025.51.4.337 ISSN 2299-8004 | e-ISSN 2353-0790 | Wydawnictwa AGH

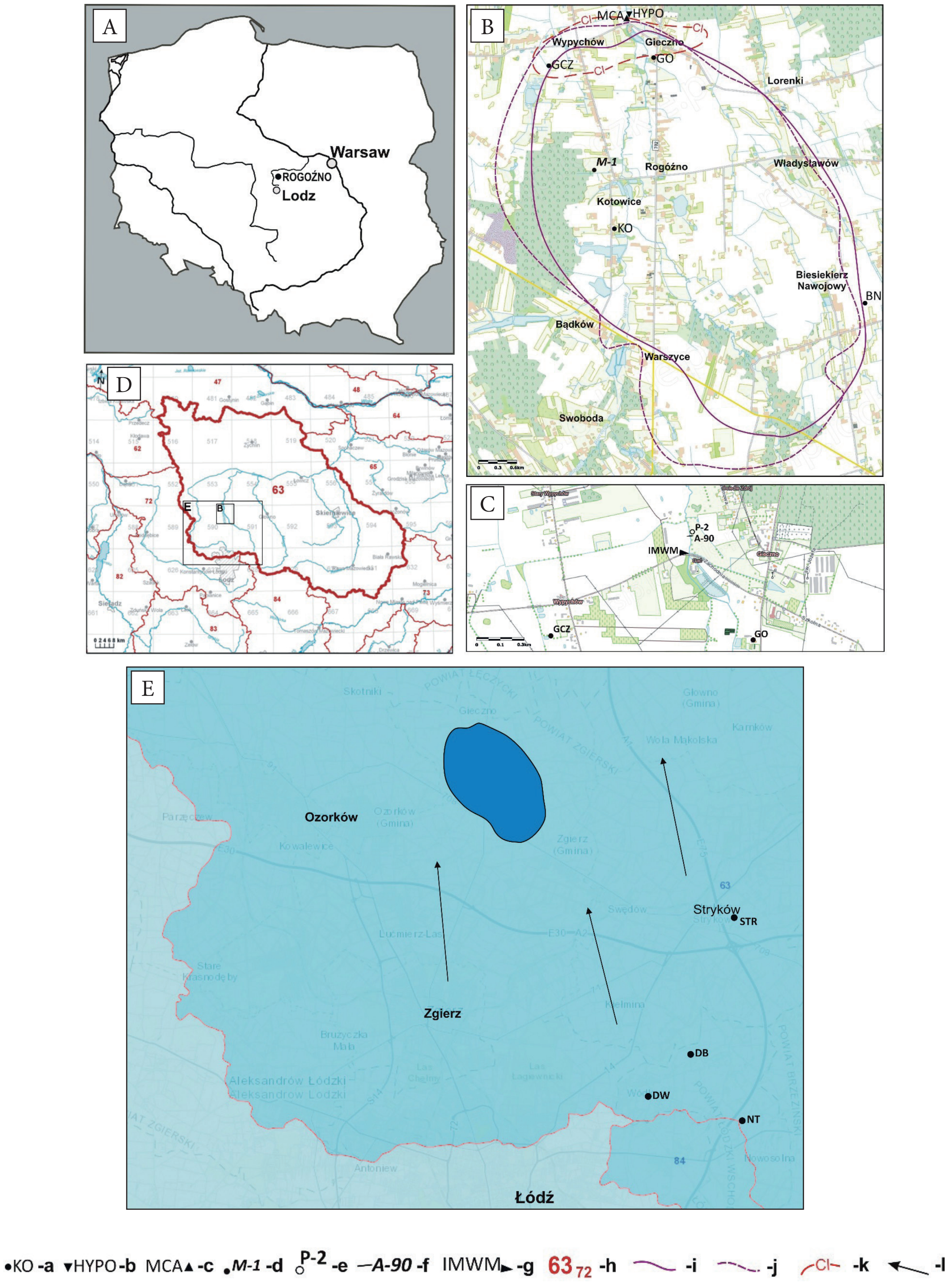

*Fig. 1. Location of the research area: A) on a national scale; B) outline of the salt dome and its clay-gypsum cap along with the location of surface and groundwater testing points; C) hyporheic water testing site; D) location of the area of interest within the boundaries of PLGW200063 (63); E) location of research wells in the PLGW200063 (63) recharge zone. Cartographic backgrounds from the Łódź Voivodeship Geoportal and for the Ground Water Body from https://geolog.pgi.gov.pl/#name=19mvaoemxx. Markings: a – research well with a marking, b – place for sampling hyporheic waters, c – place for collecting water samples from the Moszczenica River, d – well for medicinal waters (Kucharski et al. 2012), e – piezometer capturing groundwater, f – VHG measurement profile in the Moszczenica riverbed with a marking, g – IMWM water gauge station (IMWM – Institute of Meteorology and Water Management), h – marking of GWB, i – sub-Cenozoic extent of the salt dome body Rogóźno according to Dębski et al. (1963), j – the extent of the clay-gypsum cap (ibid), k – the extent of the area where the chloride concentration exceeds the requirements for drinking water (Meszczyński & Szczerbicka 2002), l – groundwater flow direction (Meszczyński & Szczerbicka 2002, Szczerbicka & Meszczyński 2002)*

They were carried out in the years 1949–1953 to identify and document the rock salt deposit in the Rogóźno diapir, piercing the overburden of Mesozoic deposits (Jaworski 1964). The local hydrogeological conditions disturbed by these works mean that brackish waters occur in this area just below the surface, already in unconfined waters. This was recognized especially in the northern part of the area marked by the contour of the salt dome on the surface (Meszczyński & Szczerbicka 2002) (Fig. 1). The modern Moszczenica riverbed runs along the long axis of this contour, draining groundwater resources in the southwestern part of PLGW200063 (Fig. 1D) (data card: https://www.pgi.gov.pl/dokumenty-pig-pib-all/psh/zadania-psh/jcwpd/jcwpd-60-79/4423-karta-informacyjna-jcwpd-nr-63/file.html), so it should be assumed that the river can also receive deep saline water from the underground catchment. Observations of vertical hydraulic gradients (VHG) between the hyporheic zone (HZ) and the Moszczenica riverbed have shown that upwelling of deep waters may occur in the river bottom (Marciniak et al. 2022, Ziułkiewicz 2022).

The aim of the research was to identify deep groundwaters forming a mixture with river waters in the HZ of Moszczenica. Therefore, research was carried out in the field of:

- identification of the VHG size and direction on the river bottom;
- hydrochemical tests to determine the presence of saline waters in the immediate vicinity of the riverbed, which required testing of groundwater occurring in the deep horizons around and above the diapir, as well as groundwater from the recharge area within PLGW200063, as well as the river waters of the Moszczenica and its hyporheic waters;
- isotope studies in the range of $^{226}$Ra and $^{228}$Ra of the above-mentioned waters.

The origin of the salinity of the Moszczenica hyporheic waters was determined by reconstructing the isotopic activity of hypothetical deep groundwaters flowing into the HZ with the actual isotopic activity of the river waters, and the isotopic activity of the waters which are the product of their mixing, i.e. waters from the HZ.

## STUDY AREA

Within the Paleozoic platform, under the cover of Mesozoic deposits, there is a thicker Zechstein deposit, developed in the salt-bearing series (Dadlez 1998). The overburden of younger rocks, which is many kilometers thick, plasticizes the salt, which is pushed upwards through all kinds of discontinuities in the overlying layers. A special role is played by tectonic deformations that occurred as a result of the Alpine orogeny movements taking place in southern Poland, although the fault zones in the Prezechstein basement indicated by Krzywiec (2006, 2009) may be of crucial importance in this respect. There is a dense network of halokinetic structures in the Łódź region (Sokołowski 1966), the most important of which is the Gopło-Ponętów-Pabianice zone (Skorupa & Dziewińska 1976). The series of diapirs developed on its basis, as an anticlinal zone, separates its north-eastern "bay" from the Mogilno-Łódź synclinorium – the so-called the Small Łódź Trough. In its northern edge, on the border with the Kutno section of the Kuyavian embankment, the Rogóźno salt diapir was formed, which was the only one in the region that broke through the overburden of Mesozoic deposits. It is the second largest salt dome in the country (Czapowski & Tarkowski 2018). The salt body was located within the zone of active groundwater circulation and was subjected to strong leaching through subrosion.

The resulting salt solutions could have moved along faults and sedimentary discontinuities. As a result of leaching 138 km$^2$ of salt, a clay-gypsum cap with a volume of 3.93 km$^3$ was formed (Małecki & Ziułkiewicz 2019). The cap is located at depths of 54.5–328.8 m, has a thickness of 12.8–286.3 m (Czapowski & Tarkowski 2018), and in the northern part it is clearly thinner than in the southern part. The clay-gypsum type of cap sediments is distributed in the plan on the edge of the salt structure, while gypsum-anhydrite sediments are concentrated in its central part (Dębski et al. 1963). Below the cap of the diapir, there is a strongly tectonically disturbed Zechstein salt series, in which the recognized profile includes: Zuber, younger rock salt, main anhydrite, plate dolomite, gray salt clay, older rock salt and older potassium salt (Czapowski & Tarkowski 2018). Older formations occur in the center of the diapir, they are internally folded and most likely surrounded by younger Zechstein series formations. The younger salt series formations in the outer zones have undergone a strong reduction. The diapir breaks through Mesozoic rocks on the border of the Kuyavian Swell and the Small Łódź Basin, hence Lower Cretaceous sediments directly adjoin it from the north-west, with Middle and Upper Cretaceous formations on the western side of the diapir and Upper Jurassic formations from the east and south (Marek 1957). The diapir cap is strongly dislocated as a result of active halokinetics and sulfate karstification. This is evidenced by the strong deformation of the overburden of Paleogene and Neogene formations (Hycnar & Ratajczak 2019) and Pleistocene clays (Kamiński 1993). The Paleogene and Neogene in the overburden of the diapir and its cap are composed of clays (sometimes carbonated), silts, quartz sands (also sometimes carbonized), as well as brown coal seams surrounded by clays. The thickness of Tertiary sediments is variable – this is the result of the presence of a number of washouts in the top of the diapir, which are filled, among others, by Miocene deposits. In such places, their thickness reaches up to 250 m. As a result of the sulfate karstification of the cap, the depositional surface of the diapir is slowly and evenly lowered. Its original structure was disturbed, and denivelations appeared on the ceiling surface, reaching several dozen meters. They became a place of accumulation of phytogenic matter, which led to the formation – in addition to thin interlayers – of two thick coal seams, an older one in the Oligocene and a younger one in the Miocene. These coals contain small amounts of chlorides, but significant amounts of $Na_2O$ and $K_2O$, which indicates their salinity. A younger coal seam is not only thicker, but also more uniform. It has a strongly folded roof surface, which is evidence of the activity of the Permian basement (Hycnar & Ratajczak 2019). In addition to leaching, halokinetics was important in deforming the roof parts of the dome, which could be activated by the transgression of ice sheets through changes in pressure on the land surface. This is indicated by the research of Piotrowski (1999) in the area of the Odra Lobe and Molewski (2007) in the Kuyavian Upland. The movement and presence of ice sheets over the Rogóźno diapir influenced the sedimentary record in Quaternary deposits. According to Jewtuchowicz (1967), this is evidenced by the number of moraine clay levels found in the overburden of the Rogóźno diapir. There are four levels there, and only one occurs in its immediate vicinity, outside the outline of the diapir. They show clear disturbances as a result of processes occurring in the overburden of the diapir (Ziułkiewicz 2022).

Interglacial erosional cuts filled with sandy formations are clearly visible at the top of individual moraine clay levels. According to Kamiński (1993), the depth of these cuts, often up to 20 m, refers to karst depressions in the clay-gypsum cap. The total thickness of the Quaternary formations above the dome ranges from 2.6 to 241.6 m (Dębski et al. 1963, Charysz 1966). The youngest series are the Moszczenica valley sediments, deposited in the erosional cutting of older formations, including the Warta clay: sands and gravels, flood mineral silts and organic sediments filling the oxbow lakes (Kamiński 1993). The modern course of the Moszczenica is the result of the karstification processes of the clay-gypsum cap and halokinesis. The degradation of the diapir cap led to the formation of a longitudinal concavity in the central part of the overburden, which determined the course of the riverbed along the longitudinal axis of the diapir contour (Fig. 1B). Further north, below the gorge section near Gieczno, where the river flows beyond the diapir, the Moszczenica does not have a developed valley, it flows in a bed formed in the recent past, as indicated by, among others, the absence of a flood terrace. Kamiński (1993) and Molewski (2014) are consistent with Lencewicz's concept (Jewtuchowicz 1967) that the river in this stretch changed its course drastically. Originally, it flowed according to the general slope of the surface to the north-west, towards Łęczyca, where it flowed into the Bzura River. The creation of the Łęczyca watershed in the Warsaw-Berlin ice-marginal valley through the activity of the Izbica-Łęczyca salt anticline (Jewtuchowicz 1967) changed its course northward, towards Piątek.

Nowadays, increased specific electrical conductivity (SEC) values and chloride ion concentrations recorded in the bottom of the Moszczenica valley are found locally (Górecki & Ziułkiewicz 2016), and the river in the section where it flows over the Rogóźno diapir does not show any signs of geogenic salinity (Górecki 2017). However, research carried out in 2017–2018 in the Moszczenica riverbed near Gieczno showed that between the river and the alluvia there are conditions favorable for intensive water exchange (Marciniak et al. 2022). Attention was paid to the possibility of ascensive inflows of deep water, which Macioszczyk (1988) considered as one of the important factors determining the chemistry of river waters. Tests conducted in 2019–2023 of river water and water collected directly from the bottom of the Moszczenica River showed the presence of hydrochemical types specific to geogenic salinity and transitional types, indicating active mixing of groundwater and river water. On this basis, the share of saline deep waters in the HZ was determined to be 18–20% (Ziułkiewicz 2022) and 33% with a longer observation series (Ziułkiewicz 2024). It was also noticed that the ascension is essentially in the central part of the bottom of the riverbed, which confirms the concept of the spatial structure of groundwater drainage in the riverbed supplied by Winter (1998).

Among the markers proposed by Gooseff (2010) used for the geochemical characterization of the hyporheic zone in previous studies, ion and SEC values were used (Ziułkiewicz 2022, 2024). However, isotopes were not used, among which isotopes of radium deserve special attention. They have been widely used to describe the interactions occurring between waters in the coastal zone (Moore 1996, 1999, 2003, Souza et al. 2010, Annett et al. 2013, Su et al. 2013), to identify the mixing of fresh and salty groundwater (Moise et al. 2000, Sturchio et al. 2001), river and underground (Eikenberg et al. 2001, Molina-Porras et al. 2020) and lake and underground sources (Kraemer 2005).

Radium isotopes are created continuously as a result of radiogenic changes $^{230}$Th, $^{232}$Th and $^{228}$Th, which belong to the series of decays of uranium and thorium. Uranium and thorium are widely distributed in nature, causing radium isotopes to continually form in all continental and oceanic sediments (Webster et al. 1995). Two isotopes are of particular importance in the study of river alimentation conditions and mixing processes: $^{226}$Ra generated in the series of decays of $^{238}$U, with a half-life $t_{1/2}$ = 1,600 years, and $^{228}$Ra generated in the series of decays of $^{232}$Th, with a half-life $t_{1/2}$ = 5.75 years. The radium isotope ratio: $^{228}$Ra/$^{226}$Ra, originating from various sequences of radiogenic transformations, should reflect the average Th/U ratio ($^{232}$Th/$^{230}$Th) in rock formations penetrated by groundwater (Porcelli & Swarzenski 2003). The correlation between $^{228}$Ra and $^{226}$Ra can be used to demonstrate the mixing of groundwater and river water due to the almost constant concentrations of both isotopes in each component of such a mixture (Eikenberg et al. 2001). According to Molina-Porras et al. (2020), this can also provide the basis for identifying the mixing ratio of water masses in different environments.

U contents and Th/U ratios are usually higher in igneous rocks and in sedimentary detrital rocks formed as a result of their erosion than in carbonate rocks, because they contain significant concentrations of U and very little Th (low Th/U ratio) (Molina-Porras et al. 2020). The contents of $^{226}$Ra and $^{228}$Ra are usually related to each other and most often small amounts of $^{228}$Ra are accompanied by small amounts of $^{226}$Ra (and *vice versa*). In waters occurring within carbonate and metamorphic sedimentary rocks, the content of radium isotopes is insignificant. In waters occurring in weathered igneous rocks, clayey sandstones and brines, this content is usually much higher (Chau & Kopeć 2010). In the case of sandstones, according to Vinson et al. (2012), what may be important for determining the activity of radium isotopes is not the basic matrix of the quartz sandstone, but the carbonate binder, such as calcite and dolomite cement.

According to Chau and Kopeć (2010), the increase in the content of radium isotopes in water is caused by the leaching of radium isotopes from water-bearing rocks, the decay of precursors (thorium isotopes) contained in the water, and the alpha-recoil process in relation to isotopes located close to the water-rock boundary, although in general, long-lived isotopes of radium are mainly introduced into water due to the dissolution of rocks, while short-lived Ra isotopes are in the alpha recoil process (Krishnaswami et al. 1982, Porcelli 2008). The reduction in the activity of radium isotopes is the result of their precipitation from water on the surfaces of aquifers and the decay of these isotopes.

In zones where there are strong changes in groundwater salinity, radium may be deposited on the surfaces of aquifers. According to Moise et al. (2000), combination of upward flow and continual mixing of groundwaters causes a gradual buildup of a radium lining on the aquifer walls and a steady-state surface activity is established. Webster (1995) notes that where there is a strong salinity gradient in estuarine river sediments, radium isotopes desorb due to ion exchange competition with major cations present in seawater. Porcelli and Swarzenski (2003) report that when radium isotopes are short-lived, they usually adapt to local conditions more quickly and over shorter distances. $^{226}$Ra, with a much longer half-life, requires a significantly greater distance to travel along the flow line to reach a given concentration in groundwater. Therefore, concentration gradients of $^{226}$Ra can be found over greater distances than in the case of the short-lived $^{228}$Ra isotopes.

## METHODS

In order to identify zones of saline water drainage into the Moszczenica bed, hydraulic gradient measurements were carried out at its bottom. Attention was focused on the stretch of the river located in the area where, according to Meszczyński and Szczerbicka (2002), chloride concentrations in groundwater exceed those required for drinking water (Fig. 1B). A gradientometer was used for the measurements (Marciniak & Chudziak 2015). This device was also used to collect water samples from the hyporheic zone to determine its physicochemical parameters as well as chemical and isotopic composition. The methodology for collecting water samples from HZ was used in previous research work carried out in the Łódź region (Ziułkiewicz et al. 2021, 2023, Ziułkiewicz 2022, 2024, Krogulec et al. 2024, Ziułkiewicz & Grulke 2024).

VHG measurements and sampling to identify hydrochemical conditions in the Moszczenica HZ in the Gieczno area have been ongoing since November 2018 (Ziułkiewicz 2022). When starting isotope research, the zone of inflow of saline waters was known. In order to select a place from which to obtain a hyporheic water sample for isotope determinations, it was necessary to: identify the upwelling and obtain the highest measured EC value in such a place (Fig. 1C). Such work was carried out for the first time on March 3, 2021. On that day, parameters were measured and samples of river water and groundwater collected by deep wells were taken in the zone above and around the diapir (Fig. 1B, C) as well as in the supply zone of PLGW200063 (Fig. 1E) (https://www.pgi.gov.pl/dokumenty-pig-pib-all/psh/zadania-psh/jcwpd/jcwpd-60-79/4423-karta-informacyjna-jcwpd-nr-63/file.html) (Table 1). The tests of water from the HZ and river waters were repeated after two years, i.e. on March 21, 2023, and were supplemented with the measurement of parameters and sampling of groundwater from the P-2 piezometer previously installed in the immediate vicinity of the Moszczenica riverbed (Fig. 1C). The work was accompanied by measurements of the flow rate of the Moszczenica River and the recording of water levels in the river at the Institute of Meteorology and Water Management (IMWM) station in Gieczno (Fig. 1C).

Measurements of physicochemical parameters of water were carried out with electrodes and sensors from Eurosensor (Poland) using the universal ELMETRON CX-742 meter (Poland), and in the piezometer and wells they were carried out using the Eijkelkamp overflow cell (Netherlands). Water samples were collected in PE containers. Chemical analyzes of water in terms of salinity measures: mineral substances (TDS), concentrations of chlorides ($Cl^-$), sulfates ($SO_4^{2-}$) and sodium cation ($Na^+$) were performed in the laboratory of the Department of Geology and Geomorphology of the Faculty of Geography Sciences of the University of Lodz and the Laboratory of Computer Analytical Techniques of the Faculty of Biology and Environmental Protection of the University of Lodz according to the standards recommended by Witczak et al. (2013). On the basis of the hydrochemical elements determined, the percentage share of saline deep water in the HZ mixture was established according to the proposals of Malard (2003) and Battin et al. (2003).

***Table 1***
*Characteristics of research points in the Rogóźno salt dome zone and in the recharge zone of PLGW200063*

| No. | Object | Acronym | Geographical coordinates N/E | Number of well* | Depth of well [m] / Age of aquifer | Filtering compartment [m] | In use |
|---|---|---|---|---|---|---|---|
| 1. | Water intake in former agricultural cooperative in Biesiekierz Nawojowy | BN | 51°57′27.8″<br>19°29′28.5″ | 5900325 | 103/Jurassic | 69.5–103.0 | no |
| 2. | Water intake in former milkcollection in Gieczno | GO | 51°58′42.6″<br>19°28′57.7″ | 5900394 | 41/Quaternary | 36.0–39.0 | no |
| 3. | “Gieczyńska” former water intake in Wypychów | GCZ | 51°59′27.6″<br>19°25′33.0″ | 5900348 | 241.4/Jurassic | 238.5–241.4 | no |
| 4. | Community water intake in Kotowice (no. 2) | KO | 51°58′06.1″<br>19°26′22.0″ | 5900594 | 53.1/Quaternary | 31.3–50.0 | yes |
| 5. | Community water intake in Dobieszków | DO | 51°50′40.6″<br>19°36′14.1″ | 5910179 | 98/Quaternary | 81.0–93.6 | yes |
| 6. | Community water intake in Dąbrowa (no. 2) | DW | 51°48′59.9″<br>19°33′42.4″ | 6280377 | 48/Quaternary | 41.0–47.0 | yes |
| 7. | Community water intake in Natolin (no. 2) | NT | 51°48′09.3″<br>19°37′43.7″ | 6280363 | 30.7/Quaternary | 88.6–101.5 | yes |
| 8. | Community water intake in Stryków (H-1) | STR | 51°54′05.4″<br>19°36′59.2″ | no data | 204/Jurassic | 72.0–204.0 | yes |
| 9. | Moszczenica River | MCA | 51°59′49.4″<br>19°26′35.5″ | – | – | – | – |
| 10. | Hyphorheic zone | HYPO | 51°59′51.9″<br>19°26′36.0″ | – | 0.2/Quaternary | 0.18–0.20 | – |
| 11. | Piezometer P-2 | P2 | 51°59′52.45″<br>19°26′36.12″ | – | 4.7/Quaternary | 2.2–4.5 | – |

* According to HYDRO Bank of Polish Geological Institute – Research Institute.

Determination of $^{226}$Ra and $^{228}$Ra were carried out in the Laboratory of Isotopic Methods at the Institute of Applied Radiation Chemistry at Lodz University of Technology. For radiometric analysis using a unique low-background spectrometry system consisting of a high-purity germanium (HPGe) detector (30% relative efficiency; CANBERRA). For analysis both isotopes radiochemical procedure of radiochemical precipitation has been applied based on instruction LMI-IN-RA2268W-02. Laboratory of Isotopic Methods apply radiochemical methods according norm ISO I7025. In radiochemical procedure chemical recovery of the method was controlled based $^{133}$Ba isotope. $^{226}$Ra isotope was analyzed based on its two progenies $^{214}$Bi (609.3, 1,120.3 and 1,764.5 keV peak energy lines) and $^{214}$Pb (2,95.2 and 351.9 keV peak energy lines). $^{228}$Ra was analyzed on the base Ac-228 isotope (911.2 and 969.0 keV peak energy line).

The results of the activity analysis of isotopes $^{226}$Ra and $^{228}$Ra were used to determine the composition of the groundwater mixture in the hyporheic zone based on the method proposed by Eikenberg et al. (2001). If two different aquifers of compositions (A) and (B) interact to form a mixed component (M), the following relationship holds, provided that two isotopes with different concentrations and isotopic ratios are available, i.e. in the case of Ra:

$$^{226}\mathrm{Ra}_{\mathrm{M}} = {}^{226}\mathrm{Ra}_{\mathrm{A}} f + {}^{226}\mathrm{Ra}_{\mathrm{B}}\,(1 - f) \tag{1}$$

$$^{228}\mathrm{Ra}_{\mathrm{M}} = {}^{228}\mathrm{Ra}_{\mathrm{A}} f + {}^{228}\mathrm{Ra}_{\mathrm{B}}\,(1 - f) \tag{2}$$

where $f$ is the fractional proportion (or “mixing factor”).

In order to hydrochemically identify the mixing of water from different aquifers occurring in the zone around the diapir and overlying the diapir was used the EMMA model, which relies on the assumptions of linearity of the mixing process, the conservative behavior of tracers, and the time invariance of end member compositions. End-members represent the chemical compositions of source waters existing within a catchment that undergo physical mixing only during travel time to the stream channel. An alternative inverse approach where eigenvector and residual analysis of observed stream water chemistry estimates the number contributing end-members. End-members characterized by direct sampling in the field are then screened for their ability to fit into the mixing space created by the analysis of observed stream water chemistry (James & Roulet 2006). For these purposes, principal component analysis (PCA) is applied. Principal component analysis is generally used in problems where the variation in a set of many, correlated variables needs to be described by a new set of few, uncorrelated variables. The new set of variables, also called the components, is sorted in decreasing order of importance, i.e., by the amount of the variation that each component explains. The general goal of PCA is to identify a small number of components that can explain a substantial portion of the variation of the original variables resulting in a lower dimensional space that explains most of the variation. The decision of how many components to retain remains subjective and is influenced by the number of input variables (Barthold et al. 2011).

According to Chistophersen and Hooper (1992), PCA is an example of "reverse" analysis because the number and composition of end elements from different environments are sought in a mixture, which in our case is hyporheic water.

# RESULTS

## Mixing of groundwater in the area of the Rogóźno salt dome

The mixing identification of water from different aquifers was based on the results of physicochemical analyzes were obtained from the HYDRO Bank of the Polish Geological Institute and are data regarding water obtained from the first pumping of the wells; they date from 1962–2007 and include 124 shots (Table 2, Fig. 2). They are the only available hydrochemical material that can be subjected to statistical processing to identify the end member mixing elements in the Rogóźno salt dome zone and its immediate surroundings. It was assumed that, despite limited reliability and representativeness, statistical analysis of a large dataset to identify general regional patterns, would to some extent limit the significance of such imperfections.

Due to the different scope of chemical data contained in the archival materials, a set of hydrochemical elements was used for the statistical analysis, which was, on the one hand, numerous, and, on the other hand, enabled access to the largest set of groundwater intakes. The selected hydrochemical elements are: pH reaction ($H^+$), total hardness (TH), oxidizability (COD-Mn), sulfates, chlorides, nitrates, nitrites, ammonium ion, iron and manganese. Purposefulness of PCA was assessed using the Bartlett and Kaiser–Meyer–Olkin tests (calculation results accordingly: $p < 0.0000001$, 0.751). Substitute variables were selected as main components, and their significant number was determined by Kaiser's rule. Factors were rotated using the VARIMAX method. The composition of substitute variables is summarized in Table 3; hydrochemical elements with high correlation ($R \geq 0.7$) with replacement variables were distinguished.

***Table 2***
*Characteristics of groundwater intakes, the data of which were used to identify potential mixing end elements in the hyporheic zone of the Moszczenica River*

| Aquifer | Number of wells | Time range of the data | Intake depth range [m b.g.l.] | Depth of well screen [m b.g.l.] |
|---|---|---|---|---|
| Upper Cretaceous | 5 | 1965–1999 | 36.0–132.0 | 29.0–120.6 |
| Upper Jurassic | 40 | 1966–2007 | 30.0–152.0 | 12.7–154.0 |
| Teritiary | 27 | 1962–2005 | 26.0–321.3 | 18.2–173.4 |
| Quaternary | 49 | 1962–2007 | 10.6–64.5 | 7.5–59.5 |

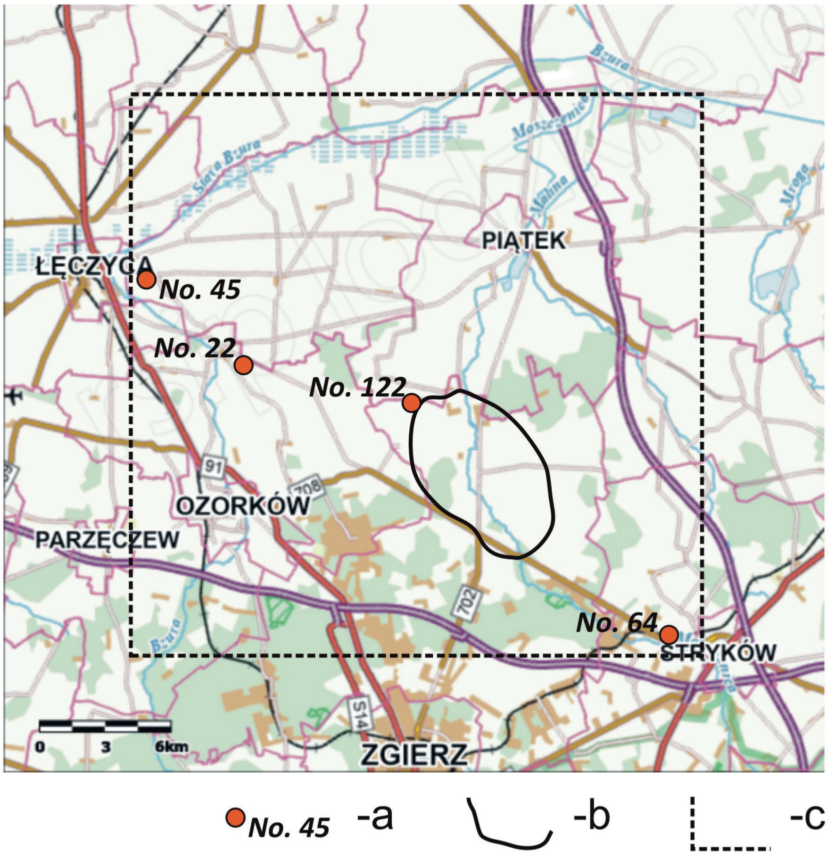

***Fig. 2.*** *Spatial range of the area where wells are located, the data of which were used for PCA. The location of the wells selected as representatives of the final elements of the groundwater mixing process in the area of the Rogóźno salt dome was indicated. Markings: a – selected well with marking, b – contour of salt dome, c – the area where the wells subjected to statistical analysis are located*

***Table 3***
*Principal components extracted from the hydrogeochemical data set of the Rogóźno salt dome area*

| Parameter | PC-1 | PC-2 | PC-3 | PC-4 |
|---|---|---|---|---|
| $H^+$ | −0.014 | −0.197 | −0.705 | −0.164 |
| Total hardness | 0.469 | 0.204 | 0.692 | 0.107 |
| $NO_3^-$ | −0.060 | −0.404 | 0.089 | 0.031 |
| $NO_2^-$ | 0.204 | 0.389 | −0.627 | 0.154 |
| $NH_4^+$ | −0.088 | 0.066 | 0.130 | 0.843 |
| $SO_4^{2-}$ | 0.768 | −0.252 | 0.234 | 0.051 |
| $Cl^-$ | 0.735 | 0.160 | −0.134 | 0.093 |
| Total Fe* | 0.034 | 0.787 | 0.265 | −0.027 |
| Total Mn** | −0.168 | 0.656 | 0.100 | 0.206 |
| COD-Mn | 0.314 | 0.007 | −0.019 | 0.709 |
| Eigenvalue | 2.133 | 1.498 | 1.295 | 1.022 |
| Cumulative contribution to explaining matrix variance [%] | 21.3 | 36.3 | 49.3 | 59.5 |

* Total Fe = $Fe^{2+} + Fe^{3+}$.

** Total Mn = $Mn^{2+} + Mn^{4+}$.

The obtained substitute variables reflect the specificity of geochemical diversity of water in terms of:

- their interactions with the salt dome and the clay and gypsum cap (PC-1);
- migration conditions of iron and manganese in an organic-rich environment in the formations of the Warsaw-Berlin ice-marginal valley and the Neogene coal levels in the overburden of the salt dome (PC-2);
- differentiation of water from Mesozoic carbonate rocks and their Cenozoic overburden (PC-3);
- differentiation of coal and non-carbon environments (PC-4).

The contribution of principal components to explaining the variance of the hydrochemical data matrix indicates that it is difficult to identify two clearly dominant hydrogeochemical conditions in this set. On the basis of the projection of the factor values onto the three-dimensional space defined by the first three principal components, a potential indication of the end member mixing elements taking place in the salt dome zone between aquifers containing normal and saline waters in the Mesozoic basement and the Cenozoic overburden was obtained (Fig. 3).

A significant number of wells are located on the line running between wells nos. 64 and 22. Well no. 22 takes water from the Upper Jurassic formations to the north-west of the diapir, and well no. 64 from the Quaternary aquifer far to the south-east of the diapir (Fig. 2). The location of the intakes selected as the representation of the final elements refers to the direction of groundwater flow in PLGW200063, from the recharge zones in the area of the Łódź Heights towards the regional drainage zone in the Warsaw-Berlin ice-marginal valley (Bierkowska 2002, Meszczyński & Szczerbicka 2002, Szczerbicka & Meszczyński 2002). The hyporheic waters of the Moszczenica are located at the top of the trapezoid, which is the projection of the end elements on the XY plane determined by PC-1 and PC-2. The statistical and hydrochemical characteristics of potential end-members and hyporheic waters are summarized in Table 4 in the order related to the direction of groundwater flow. It is related to changes in the size of PC-1 and TH. Hyporheic waters exceed end-element thresholds for PC-1 and chloride, total Mn, and $H^+$.

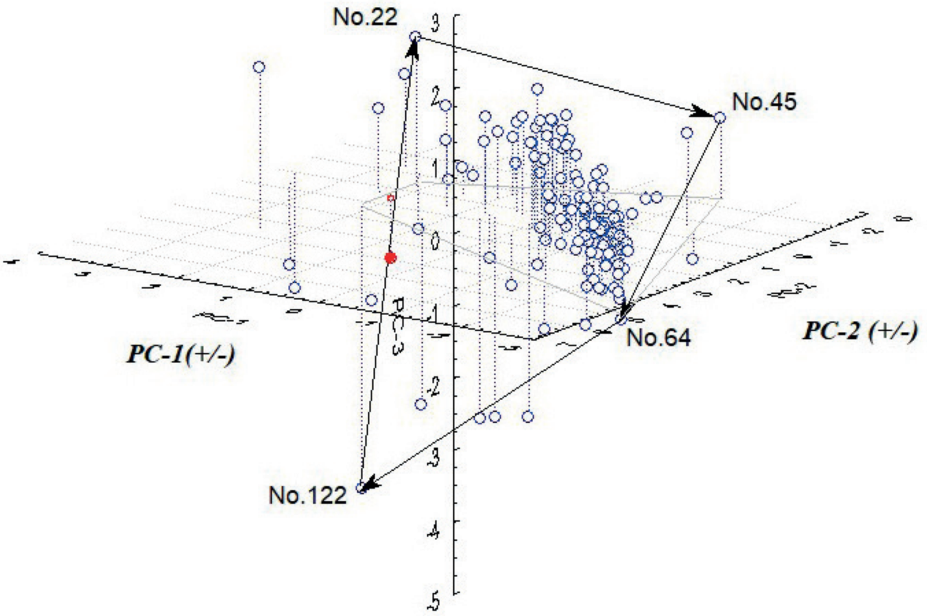

*Fig. 3. The arrangement of points representing wells in a space whose dimensions are the first three principal component. Potential end member mixing elements have been highlighted and a point (red) representing the hyporheic waters of Moszczenica River in Gieczno is marked. Note: The orientation of the chart has been optimized to make it easier to read the set of points arranged in space*

***Table 4***
*Characteristics of selected potential end member mixing elements*

| Well number/ Number acc. to HYDRO Bank | Principal components | | | Mean value of hydrochemical compounds | | | | | |
|---|---|---|---|---|---|---|---|---|---|
| | PC-1 | PC-2 | PC-3 | $SO_4^{2-}$ [mg/L] | $Cl^-$ [mg/L] | Total Fe [mg/L] | Total Mn [mg/L] | pH reaction | TH [meq/L] |
| No. 64/5910059 | −1.8272 | −0.2541 | −0.3528 | 4.0 | 12 | 2.00 | 0.10 | 7.40 | 2.70 |
| No. 122/5900348* | 2.1153 | 1.3529 | −3.9162 | 0.8 | 412 | 0.21 | 0.03 | 7.48 | 3.99 |
| No. 22/5530345 | 2.1758 | −0.4036 | 2.0421 | 221.0 | 120 | 1.18 | 0.12 | 6.64 | 8.72 |
| No. 45/5520195 | 2.5543 | 3.4296 | 2.1941 | 44.8 | 518 | 10.00 | 0.20 | 6.80 | 12.20 |
| HYPO | 3.4370 | 0.7343 | −1.1399 | 118.4 | 725 | 1.47 | 0.27 | 7.49 | 8.03 |

* No. 3 in Table 1.

## Hyporheic zone of the Moszczenica River

Measurements of the magnitude and direction of the VHG between the hyporheic zone and the riverbed were carried out on March 3, 2021 and March 21, 2023. The stage of the Moszczenica at the IMWU water gauge in Gieczno was 123 cm on the first date and 133 cm on the second date, with the Moszczenica flows being 0.655 $m^3/s$ and 0.832 $m^3/s$, respectively.

Both research dates are separated by a period of low stages in 2022 (Fig. 4), but above the average low stage, which for the water gauge in Gieczno was determined to be 120 cm (Szczepański 1995–1996).

In the studied profiles, the inflow of water from the hyporheic zone (upwelling) absolutely dominates (Fig. 5). The average VHG in the first period was slightly higher than the gradient in the second period (0.054 and 0.048 cm/cm).

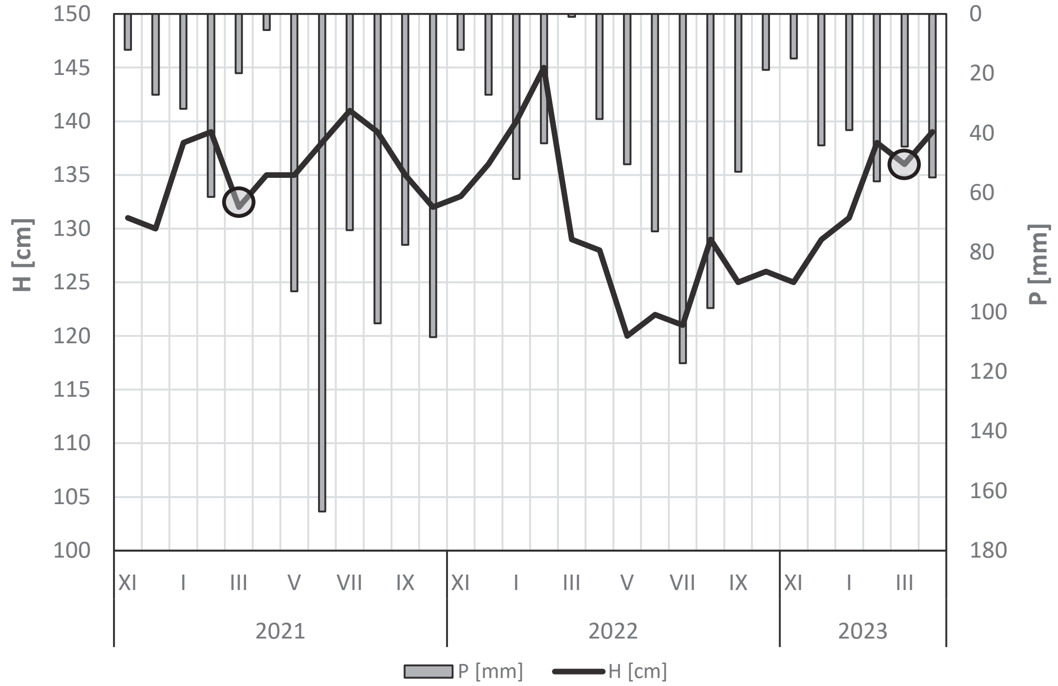

***Fig. 4.*** *Hydrometeorological conditions in the study area: average monthly water stages in the Moszczenica Rriver at the IMWM water gauge in Gieczno and monthly rainfall totals at the IMWM rainfall station in Lućmierz. The months in which water samples were taken are marked. Data: https://danepubliczne.imgw.pl/*

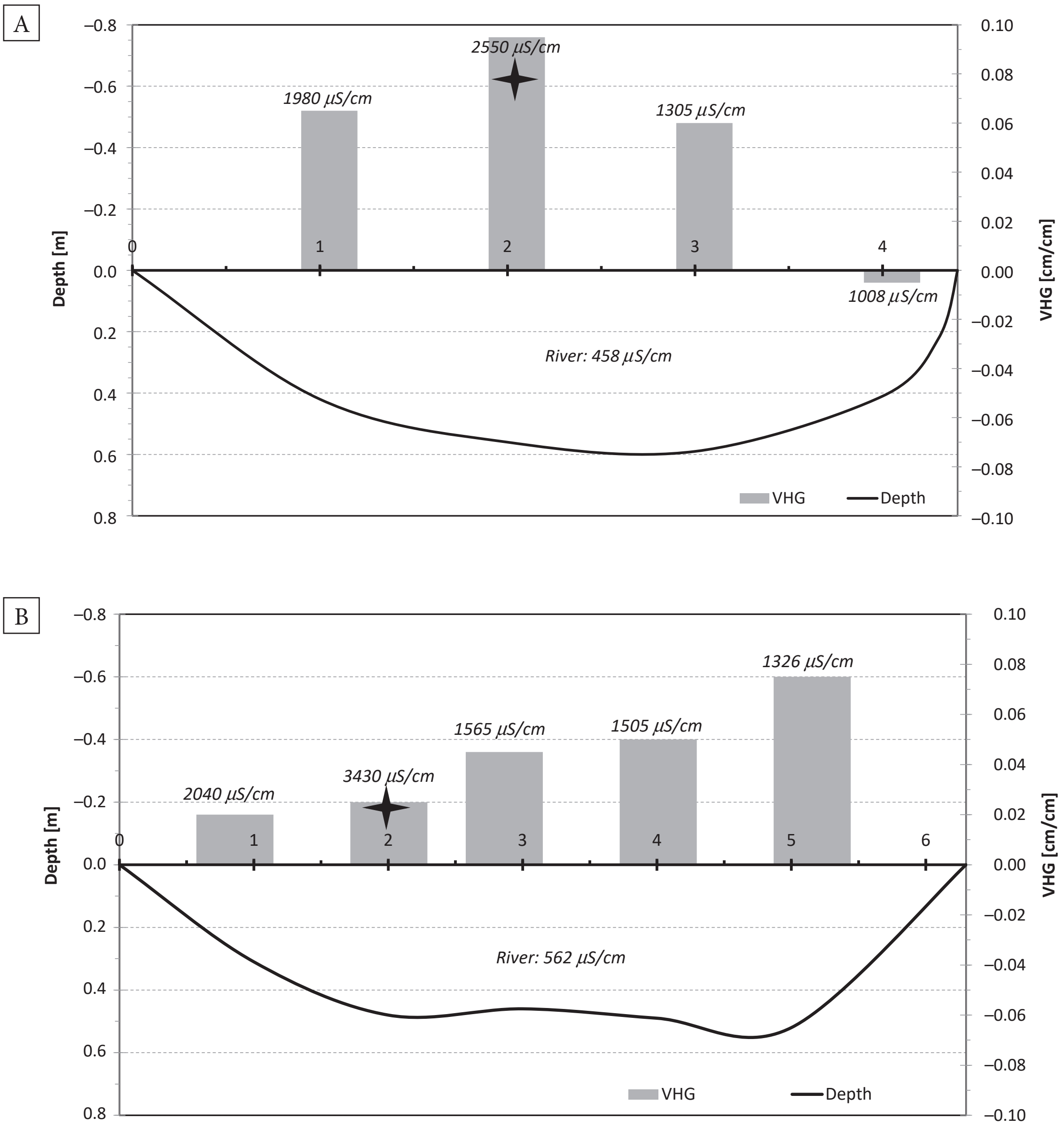

***Fig. 5.*** *Distribution of VHG values in the measurement sections of the Moszczenica riverbed at both research dates and measured EC values: A) 3.03.2021; B) 21.03.2023. Note: the asterisk indicates the places where water samples were collected for chemical analyses*

The results of chemical and isotopic analyzes of the tested waters are presented in Table 5.

The highest $^{226}$Ra activities occurred in hyporheic water (HYPO) and in the Jurassic formations surrounding the diapirs (BN and GCZ), significantly lower activities away from the diapir (STR), and the lowest in Quaternary intakes (DB, NT, DB, KO). In the case of $^{228}$Ra, the highest activity was recorded in saline Quaternary waters in the vicinity of the research site (GO) and in the water near Moszczenica (HYPO), and the lowest in municipal intakes, while no activity of the short-lived isotope was detected in the Jurassic formations away from the diapir (STR) and in one Quaternary intake in the supply zone (DW). It is noteworthy that the activity of both isotopes in the hyporheic zone was much higher than in river water and groundwater (P2).

The mutual relationship between the activity coefficients of both isotopes is shown in Figure 6A.

***Table 5***
*Values of hydrochemical elements and activities of radium isotopes in the tested waters and their activity coefficients*

| Element | BN | GO | GCZ | KO | DB | DW | NT | STR | MCA* | HYPO* | P2** |
|---|---|---|---|---|---|---|---|---|---|---|---|
| TDS [mg/L] | 532.0<br>±95.1 | 700.0<br>±105.4 | 1,060.0<br>±188.3 | 267.0<br>±42.6 | 382.0<br>±64.8 | 192.0<br>±34.5 | 155.0<br>±25.6 | 528.0<br>±94.4 | 387.0<br>241.0 | 1,480.0<br>2,158.0 | –<br>1,094.0 |
| $Cl^-$ [mg/L] | 55.5<br>±5.4 | 268.2<br>±29.1 | 219.6<br>±24.1 | 3.0<br>±0.3 | 4.2<br>±0.4 | 8.2<br>±0.8 | 9.5<br>±0.9 | 5.8<br>±0.6 | 43.5<br>32.0 | 587.3<br>862.4 | –<br>285.6 |
| $SO_4^{2-}$ [mg/L] | 13.8<br>±2.7 | 11.1<br>±2.0 | 0.8<br>±0.1 | 9.7<br>±1.9 | 15.2<br>±2.7 | 22.2<br>±4.0 | 28.0<br>±5.5 | 13.4<br>±2.7 | 38.9<br>40.9 | 147.3<br>89.5 | –<br>107.0 |
| $Na^+$ [mg/L] | 40.4<br>±2.8 | 159.7<br>±11.2 | 251.7<br>±17.6 | 5.9<br>±0.4 | 5.0<br>±0.3 | 5.7<br>±0.4 | 6.6<br>±0.5 | 6.3<br>±0.4 | 20.5<br>18.5 | 340.5<br>491.5 | –<br>69.4 |
| $^{226}Ra$ [mBq/L] | 41.4<br>±5.7 | 40.9<br>±4.8 | 43.1<br>±5.1 | 22.6<br>±2.9 | 19.8<br>±2.3 | 13.7<br>±1.5 | 19.1<br>±2.3 | 29.3<br>±3.7 | 22.0<br>18.6 | 44.4<br>45.3 | –<br>14.4 |
| $^{228}Ra$ [mBq/L] | 6.2<br>±0.9 | 31.6<br>±4.1 | 15.3<br>±1.7 | 8.4<br>±0.9 | 5.7<br>±0.8 | 0.0 | 8.4<br>±1.3 | 0.0 | 3.8<br>0.5 | 26.4<br>28.2 | –<br>9.4 |
| $^{228}Ra/^{226}Ra$ | 0.15 | 0.77 | 0.36 | 0.37 | 0.29 | 0.00 | 0.44 | 0.00 | 0.17<br>0.03 | 0.60<br>0.62 | –<br>0.66 |
| $1/^{226}Ra$ | 24.17 | 24.48 | 23.20 | 44.25 | 50.57 | 72.70 | 52.48 | 34.14 | 45.55<br>53.92 | 22.54<br>22.08 | –<br>69.43 |

* In the numerator the result from 3.03.2021, in the denominator the result from 21.03.2023.

** Only results from 21.03.2023.

The $1/^{226}Ra$ coefficient allows us to distinguish the groups of Jurassic waters around the diaphragm (BN and GCZ), saline Quaternary waters near the polygon (GO) and hyporheic waters (HYPO). The second coefficient does not provide grounds for the separation of groups, but shows the growing role of the short-lived isotope in the tested waters, with its activity culminating in the hyporheic zone and in the groundwater in its immediate surroundings (deep groundwaters – GO and unconfined groundwaters – P2) – the difference in the isotopic characteristics of water from the piezometer is noteworthy.

The relations of isotopic activity measures and hydrochemical elements presented in Figure 6 show the studied hydrogeological environment as significantly diversified, yet subject to some ordering. The amount of mineral substances shows strong covariation with $^{226}Ra$ activity (Fig. 6B). In this picture, hyporheic waters represent the boundary conditions of the relationship, and the other boundary is marked by Quaternary deep waters from the PLGW200063 recharge zone in the area of Łódź Hills (DW). The relations seem to be disturbed by the case of groundwater (P2), with too high an activity coefficient value considering the amount of minerals present in these waters. In turn, the activity ratio shows a strong relation with the sulphate index, considered to be a measure of conditions in aquifers (Pazdro & Kozerski 1990). Large amounts of sulphates may be the result of leaching of the gypsum parts of the salt diapir cap and the reduction and oxidation conditions prevailing in the underground flow path. Chlorides are the result of leaching of the salt mass. Only two of the examined cases, i.e. GCZ and GO, obtained a sulphate index value below 10, in the remaining cases, including hyporheic waters, the values are much higher. This index reached high values in waters in which the $^{228}Ra$ isotope is not active (DW and STR). However, when it is active and this activity increases relative to $^{226}Ra$, the sulfate index decreases. The case of GO waters corresponds to the highest value of the $^{228}Ra/^{226}Ra$ ratio and one of the two lowest values of the sulphate index. At the two opposite "poles" of the relationship there were Quaternary deep waters from the PLGW200063 recharge zone (i.e. DW) and saline Quaternary waters in the overlying parts, included in the immediate vicinity of the examined section of Moszczenica, i.e. GO (Fig. 1C). Between these extreme cases there are waters from Quaternary intakes in the supply area of PLGW200063 (DB, NT) and the non-saline overburden of the salt dome (KO), which constitute a completely separate group of objects. They are characterized by a low chloride content, but unlike others of the same type (DW and ST), the active isotope $^{228}Ra$.

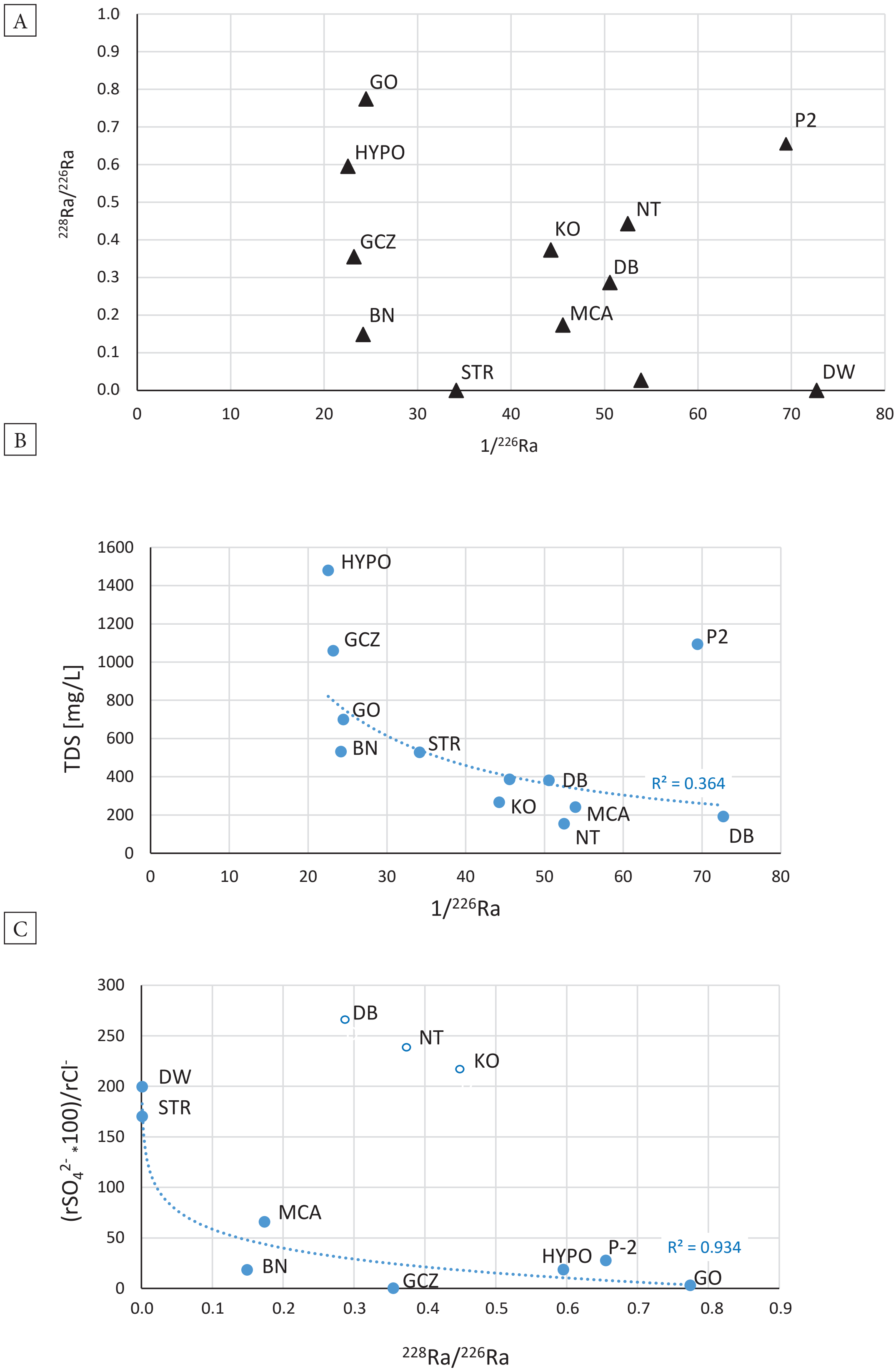

***Fig. 6.*** *Isotopic activity coefficients of the tested waters in relation to each other (A) and with mineral substances (B) and the sulphate index (C). Note: The highlighted points (empty circles) in Figures B and C were not included in the identification of trends and calculations of R2*

Preliminary assessments of the groundwater representation in the studied hyporheic zone indicated that groundwater has a share in HZ of 22%, with the rest being river waters (Ziułkiewicz 2022). Observations from the period 23.02.2023–6.03.2024 showed that this share is 33% (Ziułkiewicz 2024). Taking these shares as valid, the hypothetical activity of radium isotopes in deep waters was calculated on the basis of isotopic data from river and hyporheic waters at both research dates (B1 and B2) (Table 6). In other scenarios (B3 and B4), it was assumed (Ziułkiewicz 2024) that water from Neogene formations directly in contact with the karstified clay-gypsum cap with a known chloride and TDS content flows into the immediate vicinity of the Moszczenica riverbed (Kucharski et al. 2012). TDS and the concentration of chloride ion in river and hyporheic waters from both dates of sampling for isotope determinations were used to calculate hypothetical mixing proportions under the bottom of the Moszczenica River (Table 7).

The activities of radium isotopes and the coefficients $^{228}$Ra/$^{226}$Ra and 1/$^{226}$Ra for the B component of the hyporheic water mixture clearly differ from the size range of the tested groundwater – see Table 3. To obtain a broader reference, the simulation results were compared with literature data regarding geothermal waters of Poddębice and Uniejów (Grabowski 2012, Chau et al. 2021), waters from the Lower Cretaceous formations of the Small Łódź Trough (Grabowski et al. 2010) and other waters from the Mid-Polish Anticlinorium, Upper Silesia and the Carpathian region (Figs. 7, 8, Table 8).

The sought-for B component, in terms of its characteristics, does not have a direct equivalent in groundwater in the country, although it can be related to the waters of Iwonicz.

The graphic image of the mixing ratio in the hyporheic zone of Moszczenica with hypothetical water "B" places it between the Lower Cretaceous waters of the Mogilno-Łódź Trough, more precisely, between ordinary waters taken near Łódź for water supply purposes and geothermal waters drawn from the Lower Cretaceous formations in Uniejów (Fig. 8).

***Table 6***
*Calculation of the activity of isotopes $^{226}$Ra and $^{228}$Ra in deep groundwaters (B component) flowing into the hyporheic zone of the Moszczenica riverbed in the groundwater salinity zone*

| **Scenario** | **Mixture M (HYPO)** | | **Riverine element (MCA)** | | ***f*** | **Deep groundwaters element B (X)** | | | |
|---|---|---|---|---|---|---|---|---|---|
| | **$^{226}$Ra** | **$^{228}$Ra** | **$^{226}$Ra** | **$^{228}$Ra** | | **$^{226}$Ra** | **$^{228}$Ra** | **$^{228}$Ra/$^{226}$Ra** | **1/$^{226}$Ra** |
| | **[mBq/L]** | | | | **[–]** | **[mBq/L]** | | **[–]** | **[–]** |
| B1A | 44.4 | 26.4 | 22.0 | 3.8 | 0.22 | 123.8 | 106.5 | 0.86 | 8.08 |
| B1B | | | | | 0.33 | 80.9 | 72.3 | 0.80 | 11.13 |
| B2A | 45.3 | 28.1 | 18.5 | 0.5 | 0.22 | 140.1 | 126.2 | 0.90 | 7.14 |
| B2B | | | | | 0.33 | 99.7 | 84.3 | 0.85 | 10.03 |
| B3 | 44.4 | 26.4 | 22.0 | 3.8 | 0.13 | 194.3 | 177.6 | 0.91 | 5.15 |
| B4 | 45.3 | 28.1 | 18.5 | 0.5 | 0.20 | 152.5 | 138.7 | 0.91 | 6.57 |

***Table 7***
*Calculation the river waters share in the hyporheic zone based on analytical data of river and hyporheic waters and archival data of saline deep water according to Kucharski et al. (2012)*

| **Data** | **Chlorides [mg/L]** | | | ***f*** | **TDS [mg/L]** | | | ***f*** |
|---|---|---|---|---|---|---|---|---|
| | **River** | **HZ** | **Deep groundwaters** | | **River** | **HZ** | **Deep groundwaters** | |
| 3.03.2021 | 43.5 | 587.3 | 4,264 | 0.87 | 387 | 1,480 | 9,072 | 0.87 |
| 21.03.2023 | 32.0 | 862.4 | 4,264 | 0.80 | 241 | 2,158 | 9,072 | 0.79 |

***Fig. 7.*** *Map of chloride mineral waters and brines used as examples from literature in Table 8*

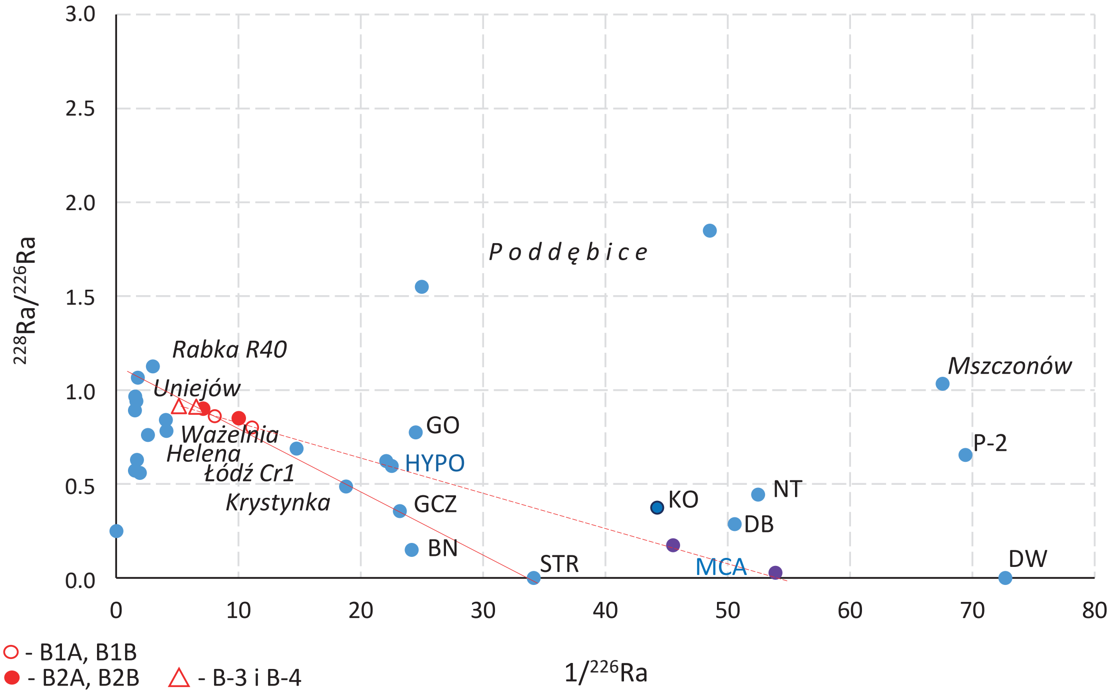

***Fig. 8.*** *Water analysis in relation to radium isotope indices with reference to regional literature data (according to Table 8) and hypothetical underground water according to various reconstruction scenarios (see Table 6)*

***Table 8***
*Comparison of the isotopic characteristics of the B component with literature data of Cl-Na type mineral waters and brines*

| **Scenario** | | **TDS [g]** | **Hydrochemical type** | **ΣRa* [mBq/L]** | **$^{228}$Ra/$^{226}$Ra* [–]** | **1/$^{226}$Ra* [–]** |
|---|---|---|---|---|---|---|
| B1A ($f$ = 0.22) | | 5.35 | – | 230.3 | 0.860 | 8.08 |
| B1B ($f$ = 0.33) | | – | – | 162.2 | 0.800 | 11.13 |
| B2A ($f$ = 0.22) | | 8.95 | – | 266.3 | 0.901 | 7.14 |
| B2B ($f$ = 0.33) | | – | – | 184.0 | 0.850 | 10.03 |
| **According to the proportions calculated in Table 5** | | | | | | |
| B3 ($f$ = 0.13) | | 8.79 | – | 371.9 | 0.914 | 5.15 |
| B4 ($f$ = 0.20) | | 8.95 | – | 291.0 | 0.911 | 6.57 |
| **Groundwater intakes** | | | | | | |
| 1. | Kotowice M-1 (Kucharski et al. 2012) | 9.07 | Cl-Na | 54.0 | – | – |
| 2. | Uniejów – min.$^{226}$Ra and $^{228}$Ra (Grabowski 2012) | – | – | 806.2 | 0.559 | 1.93 |
| 3. | Uniejów – max. $^{226}$Ra and $^{228}$Ra (Grabowski 2012) | – | – | 1,045.5 | 0.571 | 1.54 |
| 4. | Uniejów PIG/AGH-2 (Chau et al. 2021) | 6.77 | Cl-Na | 1,157 | 1.066 | 1.78 |
| 5. | Ustroń U3A (Chau et al. 2021) | 117.00 | Cl-Na-Ca | 83,700 | 0.268 | 0.015 |
| 6. | Type B of mine waters in the Upper Silesia (Chałupnik 2004) | 85.35 | – | 8,500 | 0.146 | 0.29 |
| 7. | Grudziądz IG-1 ((1)Krawiec 1999, Kozłowska et al. 2010) | 79.0 | Cl-Na(1) | 4,330 | 1.00 | 0.46 |
| 8. | Ciechocinek o-14 “Terma” ((2)Poprawski 1998, Grabowski 2012) | 44.3 | Cl-Na(2) | 1,777 | 0.664 | 0.936 |
| 9. | Sól: Warzelnia Spring (Chau et al. 2016) | 41.37 | Cl-Na | 2,520 | 0.968 | 0.78 |
| 10. | Dębowiec D-2 (Kozłowska 2010) | 32.0 | – | 2,270 | 1.12 | 0.93 |
| 11. | Rabka IG-2 (Chau et al. 2021) | 23.06 | Cl-Na | 1,178 | 0.938 | 1.64 |
| 12. | Helena (Chau et al. 2016) | 17.4 | Cl-Na | 433 | 0.781 | 4.11 |
| 13. | Warzelnia (Chau et al. 2016) | 13.1 | Cl-Na | 453 | 0.841 | 4.06 |
| 14. | Iwonicz: Elin (Chau et al. 2016) | 5.44 | Cl-Na | 242 | 0.551 | 6.41 |
| 15. | Iwonicz: Emma (Chau et al. 2016) | 4.28 | Cl-Na | 256 | 0.641 | 6.41 |
| 16. | Ciechocinek o-19a “Krystynka” ((2)Poprawski 1998, Grabowski 2012) | 3.3 | Cl-Na(2) | 81.5 | 0.487 | 18.18 |
| 17. | Siary (Chau et al. 2016) | 2.7 | Cl-Na | 299 | 0.769 | 5.91 |
| 18. | Iwonicz: Iza 19 (Chau et al. 2016) | 0.832 | Cl-Na | 101 | 0.232 | 12.19 |

* Where not specified, it was determined independently.

Water from the Jurassic formations of Stryków, Wypychów (GCZ) and Ciechocinek (“Krystynka”) are located on the extension of the proportionality line of both activity indicators. The relationship between the depth of these intakes and the activity coefficients of their waters (Fig. 9) shows that the B component could come from a depth of approx. 850–1,200 m.

With the hypothetical total mineralization (TDS) of these waters, ranging from 5.5–9.0 g/L, the hydrogeochemical gradient ranges from 0.46 g/100 m to 0.72 g/100 m, depending on the scenario. These are the lowest values in the range (0.5–26.0 g/100 m) given by Dowgiałło after Pazdro and Kozerski (1990) for Mesozoic deposits of Lowland Poland.

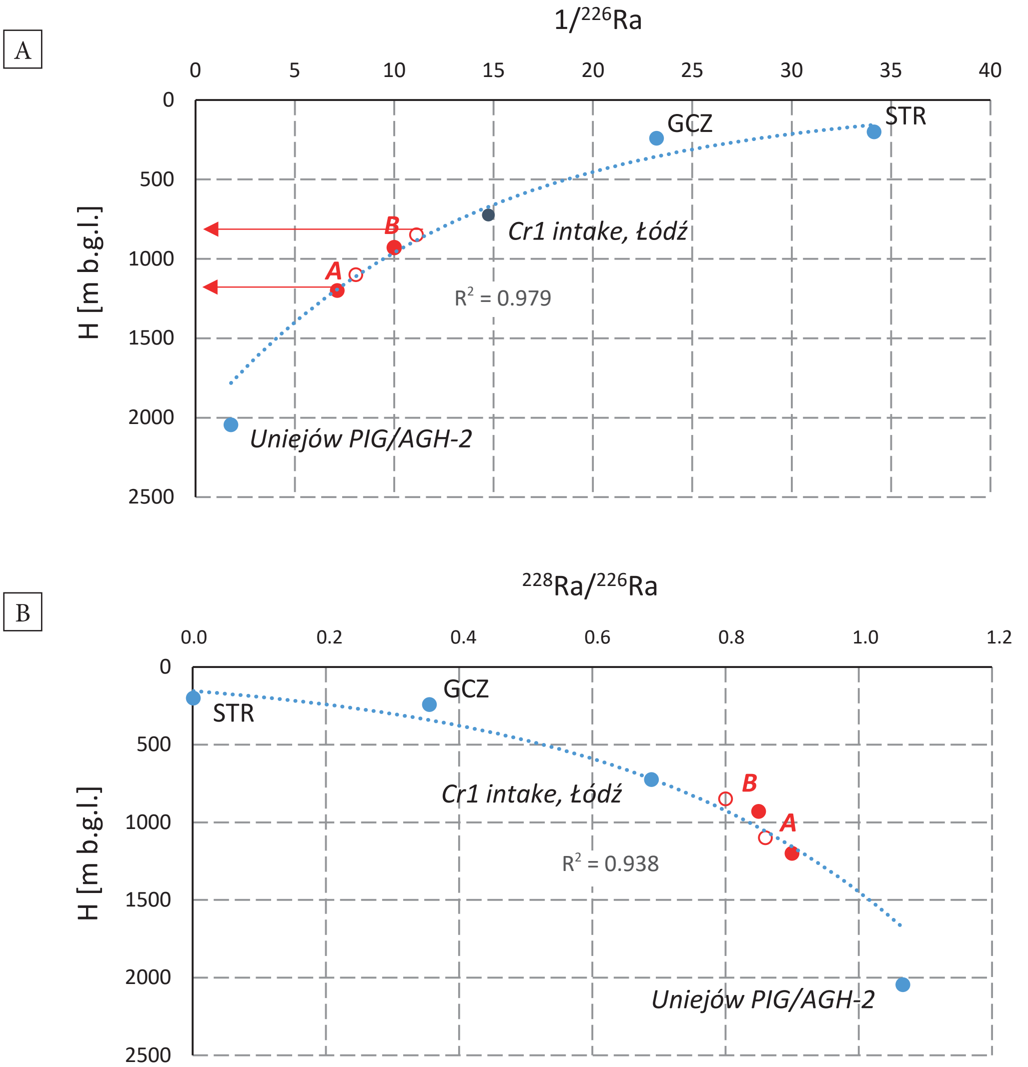

***Fig. 9.*** *The relationship between the depth of intakes in the Łódź region and the activity coefficients of radium isotopes in water coming from them: A) for 1/$^{226}$Ra; B) for $^{228}$Ra/$^{226}$Ra. Explanation of points as in Figure 8*

## DISCUSSION

The $^{226}$Ra activity of the tested waters ranges from 13.7 to 45.3 mBq/L, and two distinct groups of objects can be distinguished. The first one consists of waters with low activity – Moszczenica, groundwater from the valley bottom (P2), Quaternary municipal intakes in the recharge zone (DB and NT) and in the overburden of the salt dome (KO). The second group with almost twice as much activity – waters of the hyporheic zone, the Cenozoic saline input (GO) and groudwaters existing close to the diapir in Jurassic formations (BN and GCZ). Between these groups there are waters from the Jurassic intake in Stryków (STR). However, these are all activities much lower than those recorded by Chałupnik (2004) in the Upper Silesan brines (3,400 mBq/L), located in the lower part of the $^{226}$Ra activity range of waters flowing from the mine in the Kowary area (Chau et al. 2011), lower than those reported by Czop et al. (2013) for the Carpathian chloride waters (67–1,340 mBq/L), by Przylibski et al. (2014) for waters from the Sudetes (50–1,770 mBq/L) and Carpathians (190–620 mBq/L) and lower than in the brines of Ciechocinek (Grabowski 2012):

54.8–1,691.0 mBq/L, Grudziądz (Kozłowska et al. 2010): 2,160 mBq/L and Sopot (Kozłowska et al. 2010): 470 mBq/L. Chruścielewski and Kamiński (1999) report $^{226}$Ra activities in various aquifers taken for the needs of the Łódź waterworks. For the Upper Cretaceous, the range is 10–13 mBq/L, for the Lower Cretaceous: 10–50 mBq/L, and for the Jurassic of the Kujawy embankment: 10–23 mBq/L. Groudwaters existing close to the diapir in Jurassic formations (BN and GCZ) has $^{226}$Ra activity almost twice as high as the one reported, but the one recorded in water intake of Stryków is comparable.

The activity of $^{226}$Ra in Moszczenica is lower than that of the Vistula at the level of Płock: 27.1 mBq/L (Grabowski 2012) and Krakow: 35 mBq/L (Chałupnik et al. 2001), it is within the activity range of Kowary streams (Chau et al. 2011): 4.4–40.8 mBq/L, but it is higher than that of the Ner waters in Poddębice (Grabowski 2012): 1.20–4.68 mBq/L, or Warta in Uniejów (Grabowski 2012): 1.56–4.10 mBq/L.

The activities of $^{228}$Ra are lower than $^{226}$Ra in the tested waters, which corresponds to the situation observed by Chau et al. (2016) in Carpathian chloride-type mineral waters.

The highest $^{228}$Ra activities were recorded in oversaltdome waters in the Quaternary aquifer (GO) and in the hyporheic zone. Half the activity was found in the groundwater located close to the diapir in Jurassic formations (GCZ) and another half lower in the remaining tested waters, with the exception of the Jurassic formations of the Stryków region (ST) and the Quaternary supply zone (DW), in which the $^{228}$Ra isotope was not active. The $^{228}$Ra activity of groundwater in the Rogóźno salt dome area is much lower than the Upper Silesian brines (Chałupnik 2004): 5,100–34,700 mBq/L, but is within the lower range found in water flowing from the mine in the Kowary area (Chau et al. 2011): 14.7–6,87.0 mBq/L and the range characterizing Carpathian chloride waters (Czop et al. 2013): 8–1,240 mBq/L. However, in relation to other types of Carpathian waters (Chau et al. 2016), the tested waters most closely match the lower part of the range (or even below) given for bicarbonate waters: 12–171 mBq/L. In relation to the Ciechocinek brines (Grabowski 2012): 26.7–1,796.0 mBq/L, the waters of the Rogóźno region also correspond to the lower part of this range and are well below the $^{228}$Ra activity in the brines of Grudziądz (Kozłowska 2010): 2,170 mBq/L and Sopot (Kozłowska 2010): 1,020 mBq/L. The activity of $^{228}$Ra in Moszczenica is clearly lower than the streams in the Kowary area (Chau et al. 2011): 17.1–21.3 mBq/L, but is at the level of the Vistula in Ciechocinek (Grabowski 2012): 2.4 mBq/L, the Warta in Uniejów: 3.4–5.9 mBq/L and the Ner River in Poddębice (Grabowski 2012): 3.0–10.2 mBq/L.

Although the tested waters represent different aquifers, including surface waters, a positive covariation of radium isotope activity with the determined salinity measures was observed among them. This is consistent with the observations of, among others, Krishnaswami et al. (1991), Moise et al. (2000), Sturchio et al. (2001), Chau and Kopeć (2010), Walencik et al. (2010), Czop et al. (2013), Tomita et al. (2014), Chau et al. (2016), and Chau and Nowak (2021). The most deviating from the identified relationships (Fig. 6B and C) were unconfined groundwater (P2) and groundwater from Quaternary municipal intakes in the recharge zone (DB, NT) and the zone above the diapir (KO). In the first case, the deviations consist in a higher value of the activity coefficient $^{226}$Ra, considering the amount of mineral substances dissolved in the tested groundwater. The second case refers to waters with a low chloride content relative to sulfate concentrations and with an active isotope $^{228}$Ra, which for such anomalies is consistent with the observations of Tomita et al. (2014).

The activity ratio $^{228}$Ra/$^{226}$Ra (AR – activity ratio) in groundwater is an important instrument for estimating the genesis of Ra isotopes in groundwater (Tomita et al. 2014). At steady state, supplying radium isotopes to water through the dissolution and weathering of radium-containing minerals results in lower ARs than the $^{232}$Th/$^{238}$U activity rates of the parent aquifers due to the difference in half-lives of the two nuclides. In contrast, the delivery of Ra isotopes through the alpha-recoil process linked to the decay of Th isotopes ($^{230}$Th and $^{232}$Th) located on the rock surface has the same AR magnitudes as the $^{232}$Th/$^{238}$U activity coefficients of the parent aquifer rocks. Unfortunately, a serious difficulty in carrying out these interpretations is, as noted by Chau and Nowak (2021), the lack of data on the content of parent isotopes in Mesozoic deposits in the Polish Lowlands. Grabowski (2012) documented that in the geothermal waters of Poddębice, the factor determining radium activity is the process of its dissolution in the surrounding rocks. It should be mentioned that the value of the $^{228}Ra/^{226}Ra$ coefficient for these waters is 1.85, which is significantly higher than the tested waters (Table 6). At the same time, the ratio of $^{226}Ra/^{228}Ra$ in the tested waters is much higher than 1, which, according to Chau and Kopeć (2010), excludes the adsorption of isotopes. Therefore, if it is not dissolution and adsorption, then the mechanism that determines the high activity of radium isotopes in the tested waters, especially hyporheic waters, is desorption. Given the strong gradients of Eh and the concentrations of $Fe^{2+}$ and $Mn^{2+}$ between the hyporheic zone and river water (Ziułkiewicz 2022), it should be assumed that in the bottom sediments of Moszczenica there are conditions favorable to the sorption of radium isotopes arriving in deep water on metal oxides and hydroxides (Krishnaswami et al. 1982, Porcelli et al. 2014). However, the effectiveness of sorption may be significantly limited by the salinity of the hyporheic zone. Webster (1995) observed that where there is a strong salinity gradient in estuarine river sediments, radium isotopes desorb due to ion exchange competition with the major cations present in seawater. Tomita et al. (2014) reports that in a matrix solution with high ionic strength, the adsorption of divalent elements ($Ra^{2+}$) on the mineral surface is prevented by greater competition with monovalent elements ($Na^{+}$).

Relative differences between AR values can be used to determine the lithology of aquifers. Kraemer (2005), Vinson et al. (2012), Molina-Porras et al. (2017, 2020) note that low AR values are characteristic of carbonate environments and higher for clastic environments. In the case of the studied waters, the lowest AR values are shown by waters from Jurassic carbonate formations (STR, BN, GCZ; average 0.17), higher from Quaternary sandy formations (DW, DB, KO, NT, P2, GO; average 0.37). However, a more distinct boundary runs between waters with high chloride content (HYPO, GO, P2, GCZ) and low chloride content (DB, NT, KO, STR, BN). The average AR for the first group is 0.6, and for the second 0.21. Moszczenica with an AR of 0.03–0.17 belongs to a less salty environment; these are also values specific to river waters (Moore & Edmond 1984, Kraemer & Curwick 1991, Moore & Shaw 2008).

Comparisons of hydrochemical properties with the activities of isotopes $^{226}Ra$ and $^{228}Ra$ show that hyporheic waters are clearly similar to waters in Quaternary over diapir and Jurassic formations close to the diapir, but low compared to river waters (Fig. 6A, Table 3). It was assumed that representatives of both geochemical environments mix in the HZ. However, due to the fact that the salinity and isotope activity indices of hyporheic waters (HYPO) are higher than those of the tested groundwater, the second mixing element was not revealed by the tests. It was assumed, following Ziułkiewicz (2022, 2024), that these could be deep Oligocene aquifer in contact with the karstified gypsum-clay cap. Such mixing was simulated in order to determine the isotope activity of the hypothetical B component. Calculations were carried out in several scenarios (Table 6), which, after comparing the obtained results, indicated the possibility of the existence of such waters in the Lower Cretaceous formations of the Mogilno-Łódź Trough (Figs. 8, 9), and on a national scale – in brackish and saline Carpathian waters from Iwonicz and Rabka (Table 8).

The determined depth from which the sought B component of mixing with river water could originate, i.e. 850–1,200 m in the artesian basin. However, according to the research of Grabowski (2012) from Ciechocinek, where changes in the activity of the long-lived isotope of radium with depth were recognized in the local medicinal water intakes, the activity of the $^{226}Ra$ B component calculated in the simulation (at the level of 140–195 mBq/L) could represent water from a depth of approximately 110–180 m (Fig. 10). These are the approximate depths in the examined section of the Moszczenica valley the footwall parts of Neogene formations covering the gypsum-clay cap of the Rogóźno salt diapir.

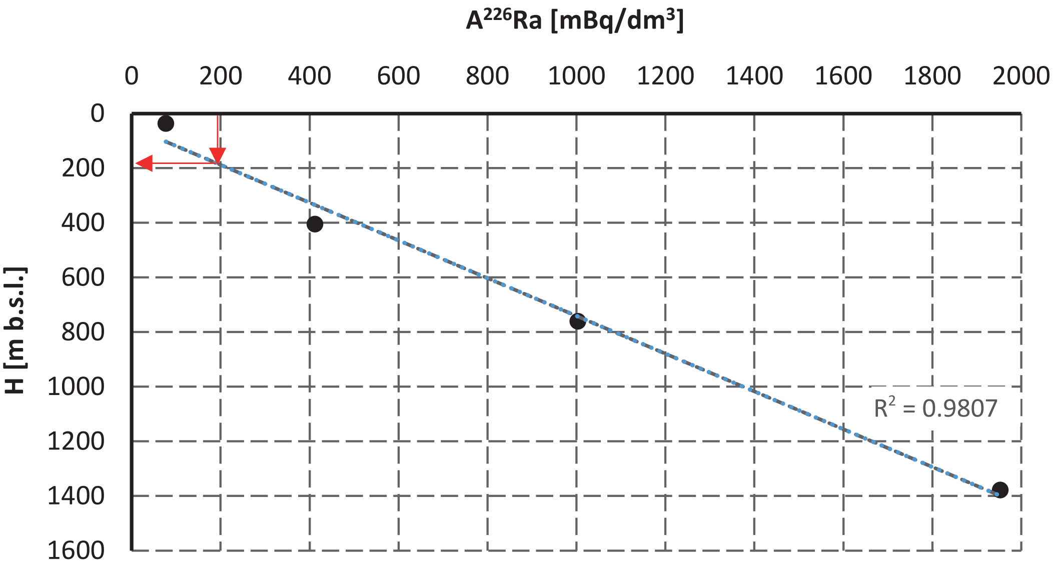

*Fig. 10.* *Relation of the calculated $^{226}$Ra activity for B component to the changes of this isotope in the groundwaters of Ciechocinek intakes (Grabowski 2012) and simulation for B component*

## CONCLUSION

The hydrogeological conditions prevailing in the overlying and surrounding area of the Rogóźno structure are more complex than in the adjacent areas. Groundwater flowing from the southeast encounters a barrier that determines the change in direction of movement towards the regional drainage base. The Moszczenica takes part in the drainage of groundwater communities, as evidenced by the presence in its hyporheic zone of waters characterized by increased mineralization and hydrochemical types typical of waters leaching the salt structure and its gypsum cap. These changes in the chemistry of groundwater occur mainly around salt dome zone.

The limited number of wells available in this area seriously limits the possibility of identifying the environments from which saline water flows into the Moszczenica. This is an intriguing research task because it transpired that HZ waters are more saline than the mixing end elements indicated in EMMA.

The reconstruction of the waters co-forming this mixture in the HZ with river waters did not supply unambiguous results. The obtained isotopic parameters fit well with the regional conditions and indicate large depths of origin of the underground component. In turn, the level of radium activity in the hypothetical deep water compared to the Ciechocinek waters shows that in the case of Rogóźno it may be at smaller depths. However, in the diapir area, the radium activity is many times lower than that found in the Moszczenica HZ.

Determining the origin of the salinizing water in the studied part of the HZ is important due to the deepening decline in river flows and a possible increase in the efficiency of drainage of the saline aquifer horizon, and thus lower dilution efficiency with dominant upwelling. The results of currently conducted hydrobiological research indicate that invertebrates inhabiting the bottom environment of the Moszczenica River in this section are responding to the geogenic salinity of the river (Płóciennik et al. 2025).

## REFERENCES

Barthold F.K., Tyralla Ch., Schneider K., Vache K.B., Frede H.-G. & Breuer F., 2011. How many tracers do we need for end member mixing analysis (EMMA)? A sensitivity analysis. *Water Resources Research*, 47(8), W08519. https://doi:10.1029/2011WR010604.

Battin T.J., Kaplan L.A., Newbold J.D. & Hendricks S.P., 2003. A mixing model analysis of stream solute dynamics and the contribution of a hyporheic zone to ecosystem function. *Freshwater Biology*, 48(6), 995–1014. https://doi.org/10.1046/j.1365-2427.2003.01062.x.

Bukowski Z., 1963. O możliwości wykorzystania solanek w okresie halsztackim na terenie Wielkopolski i Kujaw. *Archeologia Polski*, 8, 246–273.

Chałupnik S., 2004. Transfer izotopów radu z wodami kopalnianymi. *Prace Naukowe GIG. Górnictwo i Środowisko*, 2, 65–78.

Chałupnik S., Michalik B., Wysocka M., Skubacz K. & Mielnikow A, 2001. Contamination of settling ponds and rivers as a result of discharge of radium-bearing waters from Polish coal mines. *Journal of Environmental Radioactivity*, 54(1), 85–98. https://doi.org/10.1016/S0265-931X(00)00168-5.

Charysz W., 1966. O czapie gipsowo-iłowej na wysadzie solnym w Rogóźnie koło Ozorkowa. *Przegląd Geologiczny*, 14, 269–272.

Chau N.D. & Kopeć M., 2010. Czynniki określające stężenia i stosunki aktywności izotopów radu w wodach podziemnych. *Przegląd Geologiczny*, 58, 499–505.

Chau N.D. & Nowak J., 2021. Natural radioactivity in thermal waters: A case study from Poland. *Energies*, 14(3), 541. https://doi.org/10.3390/en14030541.

Chau N.D., Nowak J., Bialic M., Rajchel L., Czop M. & Wróblewski J., 2011. Nowe wyniki badań zawartości naturalnych pierwiastków promieniotwórczych w środowisku wodnym w rejonie Kowar. *Biuletyn PIG*, 445, 27–34.

Chau N.D., Kopeć M. & Nowak J., 2016. Factors controlling $^{226}$Ra, $^{228}$Ra and their activity ratio in groundwater – an application in Polish Carpathian mineral waters. *Geology, Geophysics and Environment*, 42(3), 337–351. https://doi.org/10.7494/geol.2016.42.3.337.

Chmielewska I., Chałupnik S., Wysocka M. & Smoliński A., 2020. Radium measurements in bottled natural mineral-, spring- and medicinal waters from Poland. *Water Resources and Industry*, 24, 100133. https://doi.org/10.1016/j.wri.2020.100133.

Christophersen N. & Hooper R.P., 1992. Multivariate analysis of stream water chemical data: the useof proncipal components analysis for the End-Member Mixing problem. *Water Resources Research*, 28(1), 99–107. https://doi.org/10.1029/91WR02518.

Chruścielewski W. & Kamiński Z., 1999. Radium and radon in natural underground waters supply in the region of Łódź, Poland. *International Journal of Occupational Medicine and Environmental Health*, 12(3), 229–238.

Czapowski G. & Tarkowski R., 2018. Uwarunkowania geologiczne wybranych wysadów solnych w Polsce i ich przydatność do budowy kawern do magazynowania wodoru. *Biuletyn PIG*, 472, 53–82.

Czop M., Chau N.D., Rajchel L., Rajchel J. & Motyka J., 2013. Występowanie izotopów uranu i radu w karpackich wodach chlorkowych. *Biuletyn PIG*, 456(14/1), 89–96.

Dadlez R., 1998. *Mapa tektoniczna kompleksu cechsztyńsko-mezozicznego na Niżu Polskim. 1:500 000.* Wydawnictwa Geologiczne, Warszawa.

Dębski J., 1963. *Dokumentacja geologiczna złoża soli kamiennej w wysadzie solnym Łanięta, gmina Łanięta, pow. Kutno, woj. Łódź.* Narodowe Archiwum Geologiczne, Warszawa [unpublished].

Eikenberg J., Triccab A., Vezzua G., Stilleb P., Bajoa S. & Ruethia M., 2001. $^{228}$Ra/$^{226}$Ra/$^{224}$Ra and $^{87}$Sr/$^{86}$Sr isotope relationships for determining interactions between ground and river water in the upper Rhine valley. *Journal of Environmental Radioactivity*, 54(1), 133–162. https://doi.org/10.1016/S0265-931X(00)00171-5.

Gooseff M.N., 2010. Defining hyporheic zones – advancing our conceptual and operational definitions of where stream water and groundwater meet. *Geography Compass*, 4(8), 945–955. https://doi.org/10.1111/j.1749-8198.2010.00364.x.

Górecki M. & Ziułkiewicz M., 2016. The presence of geogenically saline waters in the area of salt dome Rogóźno (central Poland). *Geology, Geophysics and Environment*, 42(3), 289–310. https://doi.org/10.7494/geol.2016.42.3.289.

Grabowski P., 2012. *Radiologiczna ocena przydatności polskich wód geotermalnych do celów pitnych i balneologicznych*. Politechnika Łódzka, Łódź [Ph.D. thesis].

Grabowski P., Długosz M., Szajerski P. & Bem H., 2010. A comparison of selected natural radionuclide concentrations in the thermal groundwater of Mszczonów and Cieplice with deep well water from Łódź city, Poland. *Nukleonika*, 55(2), 181–185.

Hycnar E. & Ratajczak T., 2019. Ewaporaty solne a polskie złoża węgla brunatnego. [in:] Lewicka E. (red.), *Aktualia i perspektywy gospodarki surowcami mineralnymi*, Wydawnictwo IGSMiE PAN, Kraków, 191–207.

James A.L. & Roulet N.T., 2006. Investigating the applicability of end-member mixing analysis (EMMA) across scale: A study of eight small, nested catchments in a temperate forested watershed. *Water Resources Research*, 42(8), W08434. https://doi.org/10.1029/2005WR004419.

Jaworski A., 1964. Powierzchniowe przejawy zasolenia na obszarze wysadu solnego w Rogóźnie koło Łodzi. *Przegląd Geologiczny*, 12, 148–149.

Jewtuchowicz S., 1967. *Geneza pradoliny warszawsko-berlińskiej między Nerem i Moszczenicą*. Prace Geograficzne – Polska Akademia Nauk. Instytut Geografii, 62, Wydawnictwa Geologiczne, Warszawa.

Jodłowski A., 1977. Badania archeologiczne nad początkami eksploatacji soli w Polsce Środkowej. *Sprawozdania Archeologiczne*, 29, 179–187.

Kamiński J., 1993. *Późnoplejstocenska i holoceńska transformacja doliny Moszczenicy*. Acta Geographica Lodziensia, 64, Łódzkie Towarzystwo Naukowe, Łódź.

Kozłowska B., Walencik A., Przylibski T.A., Dorda J. & Zipper W., 2010. Uranium, radium and radon isotopes in selected brines of Poland. *Nukleonika*, 55(4), 519–522.

Kraemer T.F., 2005. Radium isotopes in Cayuga Lake, New York: Indicators of inflow and mixing processes. *Limnology and Oceanography*, 50(1), 158–168. https://doi.org/10.4319/lo.2005.50.1.0158.

Kraemer T.F. & Curwick P.B., 1991. Radium isotopes in the lower Mississippi River. *Journal of Geophysical Research. Oceans*, 96(C2), 2797–2806. https://doi.org/10.1029/90JC02456.

Krishnaswami S., Graustein W.C., Turekian K.K., Dowd F., 1982. Radium, thorium, and radioactive lead isotopes in groundwaters: Application to the in-situ determination of adsorption-desorption rate constants and retardation factors. *Water Resources Restoration*, 18(6), 1663–1675. https://doi.org/10.1029/WR018i006p01663.

Krishnaswami S., Bhushan R. & Baskaran M., 1991. Radium isotopes and $^{222}$Rn in shallow brines, Kharaghoda (India). *Chemical Geology: Isotope Geoscience section*, 87(2), 125–136. https://doi.org/10.1016/0168-9622(91)90046-Y.

Krzywiec P., 2006. Tektonika solna na Niżu Polskim – wnioski z interpretacji danych sejsmicznych. *Przegląd Geologiczny*, 54, 303–304.

Krzywiec P., 2009. Geometria i ewolucja wybranych struktur solnych z obszaru Niżu Polskiego w świetle danych sejsmicznych. *Przegląd Geologiczny*, 57, 812–818.

Kucharski M., Sokołowski A. & Olczak M. 2012. *Dokumentacja hydrogeologiczna ustalająca zasoby eksploatacyjne złoża wód do celów leczniczych z osadów górnego oligocenu ujętych otworem M-1 w Kotowicach*. Narodowe Archiwum Geologiczne, Warszawa [unpublished].

Macioszczyk A., 1988. Chemizm wód podziemnych dolin rzecznych oraz główne czynniki kształtujące go. *Zeszyty Problemowe Postępów Nauk Rolniczych*, 347, 205–220.

Malard F., 2003. Groundwater-surface water interactions. [in:] Ward J.V. & Uehlinger U. (eds.), *Ecology of a Glacial Flood Plain*, Aquatic Ecology Series, 1, Springer, Dordrecht, 37–56. https://doi.org/10.1007/978-94-017-0181-5_3.

Marciniak M., Ziułkiewicz M. & Górecki M., 2022. Variability of water exchange in the hyporheic zone of a lowland river in Poland based on gradientometric studies. *Quaestiones Geographicae*, 41(3), 143–158. https://doi.org/10.2478/quageo-2022-0030.

Marek S., 1957. Wstępne rozpoznanie stratygraficzne dolnej kredy w obszarze Rogóźna i Ozorkowa. *Geological Quarterly*, 1, 247–258.

Meszczyński J. & Szczerbicka M., 2002. *Mapa hydrogeologiczna Polski 1:50 000. Arkusz Zgierz (590)*. Państwowy Instytut Geologiczny, Warszawa.

Moise T., Starinsky A., Katz A. & Kolodny Y., 2000. Ra isotopes and Rn in brines and ground waters of the Jordan-Dead Sea Rift Valley: Enrichment, retardation, and mixing. *Geochimica et Cosmochimica Acta*, 64(14), 2371–2388. https://doi.org/10.1016/S0016-7037(00)00369-0.

Molewski P., 2007. *Neotektoniczne i glacidynamiczne uwarunkowania wykształcenia plejstocenu Wysoczyzny Kujawskiej*. Wydawnicto Naukowe UMK, Toruń.

Molewski P., 2014. Paleogeograficzne uwarunkowania odpływu wód z zastoiska warszawskiego doliną Bachorzy i pradoliną warszawsko-berlińską w czasie stadiału głównego zlodowacenia Wisły. *Landform Analysis*, 25, 105–114. http://doi.org/10.12657/landfana.025.009.

Molina-Porras A., Condomines M. & Seidela J.L., 2017. Determination of low-level Radium isotope activities in fresh waters by gamma spectrometry. *Applied Radiation and Isotopes*, 120, 119–125. https://doi.org/10.1016/j.apradiso.2016.12.010.

Molina-Porras A., Condomines M., Legeay P.L., Bailly-Comte V. & Seidel J.L., 2020. Radium isotopes as a tracer of water sources and mixing in the Vidourle Stream (South of France). *Aquatic Geochemistry*, 26(2), 119–136. https://doi.org/10.1007/s10498-020-09371-1.

Moore W.S., 1996. Large groundwater inputs to coastal waters revealed by $^{226}$Ra enrichments. *Nature*, 380, 612–614. https://doi.org/10.1038/380612a0.

Moore W.S., 1999. The subterranean estuary: A reaction zone of ground water and sea water. *Marine Chemistry*, 65(1–2), 111–126. https://doi.org/10.1016/S0304-4203(99)00014-6.

Moore W.S., 2003. Sources and fluxes of submarine groundwater discharge delineated by radium isotopes. *Biogeochemistry*, 66(1–2), 75–93. https://doi.org/10.1023/B:BIOG.0000006065.77764.a0.

Moore W.S. & Edmond J.M., 1984. Radium and barium in the Amazon River system. *Journal of Geophysical Research*, 89(C2), 2061–2065. https://doi.org/10.1029/JC089iC02p02061.

Moore W.S. & Shaw T.J., 2008. Fluxes and behavior of radium isotopes, barium, and uranium in seven Southeastern US rivers and estuaries. *Marine Chemistry*, 108(3–4), 236–254. https://doi.org/10.1016/j.marchem.2007.03.004.

Pazdro Z. & Kozerski B., 1990. *Hydrogeologia ogólna*. Wydawnictwa Geologiczne, Warszawa.

Piotrowski A., 1999. Wpływ zróżnicowanego obciążenia strefy krawędziowej lądolodu na migrację soli. *Przegląd Geologiczny*, 47, 1016–1020.

Płóciennik M., Jóźwiak P., Długosz-Lisiecka M., de Mendoza G., Hodunko R., Brodecki J., Matera T., Słomczyński M., Tończyk G., Jabłońska A., Zawadzki W., Wrona W., Sławska A., Kaczorowski D., Młynarczyk M. & Ziułkiewicz M., 2025. Zasolenie geogeniczne wód rzecznych a bentos – szczególny przypadek rzeki Moszczenicy. [in:] *Od molekuł do ekosystemów – współczesne badania w hydrobiologii: Streszczenia: XXVI Zjazd Hydrobiologów Polskich: Szczecin 16–19 września 2025 roku*, Wydawnictwo Naukowe Uniwersytetu Szczecińskiego, Szczecin, 89.

Porcelli D., 2008. Investigating groundwater processes using U- and Th-series nuclides. [in:] Krishnaswami S. & Cochran J.K. (eds.), *U-Th Series Nuclides in Aquatic Systems*, Elsevier, New York, 105–153.

Porcelli D. & Swarzenski P.W., 2003. The behavior of U-and Th-series nuclides in groundwater. *Reviews in Mineralogy and Geochemistry*, 52(1) 317–361. https://doi.org/10.2113/0520317.

Porcelli D., Kim C.K., Martin P., Moore W.S. & Phaneuf M., 2014. Properties of radium. [in:] *The Environmental Behaviour of Radium: Revised Edition*, IAEA Technical Reports Series, 476, International Atomic Energy Agency, Vienna, 6–32.

Przylibski T.A., Gorecka J.,Kula A., Fijałkowska-Lichwa L., Zagożdżon K., Zagożdżon P., Miśta W. & Nowakowski R., 2014. $^{222}$Rn and $^{226}$Ra activity concentrations in groundwaters of southern Poland: new data and selected genetic relations. *Journal of Radioanalytical and Nuclear Chemistry*, 301(3), 757–764. https://doi.org/10.1007/s10967-014-3215-x.

Skorupa J. & Dziewińska L., 1976. Kompleksowa interpretacja wyników badań geofizycznych dla strefy Gopło-Pabianice ze szczególnym uwzględnieniem utworów cechsztynu i podłoża. *Kwartalnik Geologiczny*, 20, 137–156.

Sokołowski J., 1966. *Rola halokinezy w rozwoju osadów mezozoicznych i kenozoicznych struktury Mogilna i synklinorium mogileńsko-łódzkiego*. Wydawnictwa Geologiczne, Warszawa.

Souza T.A., Godoy J.M., Godoy M.L., Moreira I., Caralho Z.L., Salomao M.S. & Rezende C.E., 2010. Use of myltitracers for the study of water mixing in the Paraiba do Sul River estuary. *Journal of Environmental Radiactivity*, 101(7), 564–570. https://doi.org/10.1016/j.jenvrad.2009.11.001.

Sturchio N.C., Banner J.L., Binz C.M., Heraty L.B. & Musgrove M., 2001. Radium geochemistry of ground waters in Paleozoic carbonate aquifers, midcontinent, USA. *Applied Geochemistry*, 16(1), 109–122. https://doi.org/10.1016/S0883-2927(00)00014-7.

Su N., Du J., Li Y. & Zhang J., 2013. Evaluation of surface water mixing and associated nutrient fluxes in the East China Sea sing $^{226}$Ra and $^{228}$Ra. Marine *Chemistry*, 156, 108–119. https://doi.org/10.1016/j.marchem.2013.04.009.

Szczerbicka M. & Meszczyński J., 2002. *Mapa hydrogeologiczna Polski. Arkusz Głowno (591)*. Państwowy Instytut Geologiczny, Warszawa.

Tomita J., Zhang J. & Yamamoto M., 2014. Radium isotopes ($^{226}$Ra and $^{228}$Ra) in NaCl type groundwaters from Tohoku District (Aomori, Akita and Yamagata Prefectures) in Japan. *Journal of Environmental Radioactivity*, 137, 204–212. https://doi.org/10.1016/j.jenvrad.2014.07.021.

Vinson D.S., Lundy J.R., Dwyer G.S. & Vengosh A., 2012. Implications of carbonate-like geochemical signatures in a sandstone aquifer: Radium and strontium isotopes in the Cambrian Jordan aquifer (Minnesota, USA). *Chemical Geology*, 334, 280–294. https://doi.org/10.1016/j.chemgeo.2012.10.030.

Webster I.T., Hancock G.J. & Murray A.S., 1995. Modelling the effect of salinity on radium desorption from sediments. *Geochimica et Cosmochimica Acta*, 59(12), 2469–2476. https://doi.org/10.1016/0016-7037(95)00141-7.

Winter T.C., Harvey J.W., Franke O.L. & Alley W.M., 1998. *Ground Water and Surface Water: A Single Resource*. Circular, 1139, U.S. Geological Survey, Denver.

Ziułkiewicz M., 2022. Salinization of the Moszczenica river's hyporheic zone in the vicinity of the Rogóźno salt dome. *Acta Geographica Lodziensia*, 112, 163–184. https://doi.org/10.26485/AGL/2022/112/10.

Ziułkiewicz M., 2024. Underwater chemical denudation expressions of the Rogóźno salt dome on the example of the Moszczenica riverbed stretch in Gieczno. *Acta Geographica Lodziensia*, 116, 121–138. https://doi.org/10.26485/AGL/2024/116/7.

Ziułkiewicz M. & Grulke R., 2024. Hydrochemical aspects of water exchange through the bottom of headwater stream in suburban zone on the example of the Malina watercourse in Zgierz (Central Poland). *Geology, Geophysics and Environment*, 50(3), 231–251. https://doi.org/10.7494/geol.2024.50.3.231.

Ziułkiewicz M., Grulke R. & Gajda N., 2021. Identyfikacja dopływu substancji biogennych ze strefy hyporeicznej do koryta cieku źródliskowego na obszarze podmiejskim. [in:] Czerniawski R. & Bilski P. (red.), *Funkcjonowanie i ochrona wód płynących*, Volumina.pl Daniel Krzanowski, Szczecin, 263–281.

Ziułkiewicz M., Fortuniak A., Górowski J., Ajzert M., Kaźmierczak K., Lik K., Mytkowska N. & Ślusarczyk T., 2023. Zintegrowana ocena stanu hydrochemicznego doliny rzecznej w obszarze podmiejskim na przykładzie Strugi Dobieszkowskiej (Młynówki) (gm. Stryków Acta Universitatis Lodziensis). *Folia Geographica Physica*, 22, 19–36. https://doi.org/10.18778/1427-9711.22.02.

Zukin J.G., Hammond D.E., Ku T.L. & Elders W.A., 1987. Uranium-thorium series radionuclides in brines and reservoir rocks from two deep geothermal boreholes in the Salton Sea Geothermal Field, southeastern California. *Geochimica et Cosmochimica Acta*, 51(10), 2719–2731. https://doi.org/10.1016/0016-7037(87)90152-9.